Received: 21 November 2023 | Revised: 18 June 2024 | Accepted: 12 July 2024

DOI: 10.1002/ecy.4402

ARTICLE

ECOLOGY
ECOLOGICAL SOCIETY OF AMERICA

Special Feature: Advancing spectral biology to understand plant diversity across scales

# Seasonal timing of fluorescence and photosynthetic yields at needle and canopy scales in evergreen needleleaf forests

**Zoe Amie Pierrat**[1,2] | **Troy Magney**[3] | **Andrew Maguire**[2] | **Logan Brissette**[3] | **Russell Doughty**[4] | **David R. Bowling**[5] | **Barry Logan**[6] | **Nicholas Parazoo**[2] | **Christian Frankenberg**[7] | **Jochen Stutz**[1]

[1]Department of Atmospheric and Oceanic Sciences, University of California Los Angeles, Los Angeles, California, USA

[2]Jet Propulsion Laboratory, California Institute of Technology, Pasadena, California, USA

[3]Department of Plant Sciences, University of California Davis, Davis, California, USA

[4]College of Atmospheric and Geographic Sciences, University of Oklahoma, Norman, Oklahoma, USA

[5]School of Biological Sciences, University of Utah, Salt Lake City, Utah, USA

[6]Biology Department, Bowdoin College, Brunswick, Maine, USA

[7]Division of Geological and Planetary Sciences, California Institute of Technology, Pasadena, California, USA

**Correspondence**
Zoe Amie Pierrat
Email: zoe.a.pierrat@jpl.nasa.gov

**Funding information**
National Aeronautics and Space Administration (Postdoctoral Program Fellowship), Grant/Award Numbers: 80NSSC19M0133, NNN12AA01C; National Science Foundation, Grant/Award Number: 1926090; National Science Foundation, Grant/Award Number: 1929709; National Science Foundation Graduate Research Fellowship, Grant/Award Numbers: DGE-1650604, DGE2034835

## Abstract

The seasonal timing and magnitude of photosynthesis in evergreen needleleaf forests (ENFs) has major implications for the carbon cycle and is increasingly sensitive to changing climate. Earlier spring photosynthesis can increase carbon uptake over the growing season or cause early water reserve depletion that leads to premature cessation and increased carbon loss. Determining the start and the end of the growing season in ENFs is challenging due to a lack of field measurements and difficulty in interpreting satellite data, which are impacted by snow and cloud cover, and the pervasive "greenness" of these systems. We combine continuous needle-scale chlorophyll fluorescence measurements with tower-based remote sensing and gross primary productivity (GPP) estimates at three ENF sites across a latitudinal gradient (Colorado, Saskatchewan, Alaska) to link physiological changes with remote sensing signals during transition seasons. We derive a theoretical framework for observations of solar-induced chlorophyll fluorescence (SIF) and solar intensity-normalized SIF ($SIF_{relative}$) under snow-covered conditions, and show decreased sensitivity compared with reflectance data (~20% reduction in measured SIF vs. ~60% reduction in near-infrared vegetation index [NIRv] under 50% snow cover). Needle-scale fluorescence and photochemistry strongly correlated ($r^2 = 0.74$ in Colorado, 0.70 in Alaska) and showed good agreement on the timing and magnitude of seasonal transitions. We demonstrate that this can be scaled to the site level with tower-based estimates of $LUE_P$ and $SIF_{relative}$ which were well correlated across all sites ($r^2 = 0.70$ in Colorado, 0.53 in Saskatchewan, 0.49 in Alaska). These independent, temporally continuous datasets confirm an increase in physiological activity prior to snowmelt across all three evergreen forests. This suggests that data-driven and process-based carbon cycle models which assume negligible physiological activity prior to snowmelt are inherently flawed, and underscores the utility

**Handling Editor:** Jeannine Cavender-Bares

of SIF data for tracking phenological events. Our research probes the spectral biology of evergreen forests and highlights spectral methods that can be applied in other ecosystems.

**KEYWORDS**
carbon cycle, evergreen needleleaf forests (ENFs), PAM-fluorimetry, phenology, photosynthesis, remote sensing, solar-induced fluorescence (SIF), spectral biology

## INTRODUCTION

Evergreen needleleaf forests (ENFs) are a major contributor to the global carbon and water cycles and are one of the vegetation types most sensitive to environmental change (Bonan, 2008; Thurner et al., 2014). Climate change has led to warmer spring temperatures and longer potential growing seasons in many ENFs, but the impacts of this change on boreal annual carbon balance and seasonal vegetation phenology remain uncertain (Fisher et al., 2018; Fu et al., 2017; Goetz et al., 2005; Richardson et al., 2010; Schaefer et al., 2014). Specifically, the onset and cessation of photosynthetic carbon uptake (gross primary productivity, GPP) is a major factor that determines the response of ENFs to climate. Many models work under the assumption that springtime carbon uptake begins following snowmelt, which suggest a substantial increase in $CO_2$ uptake following earlier snowmelt dates (Pulliainen et al., 2017). Despite this importance, quantifying start and end of season dates has remained challenging, with large disagreements between measurements and models (Hu et al., 2010; Jeong et al., 2011, 2017; Parazoo et al., 2018). This can be attributed to the unique set of challenges posed by complex evergreen ecophysiology and northern high latitude climates where most ENFs are located, emphasizing a need for high spatiotemporal resolution observations of these ecosystems to validate and understand coarse satellite observations (Nelson et al., 2022).

Long-term, continuous ground observations of carbon fluxes from towers are both challenging to conduct and represent limited spatial coverage in ENFs, particularly in high-latitude systems. While eddy-covariance measurements provide our best estimate of the timing and magnitude of GPP at the canopy scale, they are prone to uncertainty, particularly during the spring and fall transition seasons when initial fluxes can be especially small relative to growing-season maximums (Baldocchi, 2003; Hollinger & Richardson, 2005). Both needle-scale measurements of photochemistry and canopy remote sensing are a necessary bridge for understanding and tracking phenological change. Greenness-based remote sensing of phenology using indices such as NDVI are ineffective in evergreen vegetation (Dye & Tucker, 2003; Magney, Bowling, et al., 2019; Magney, Frankenberg, et al., 2019; Pierrat et al., 2021; Sims et al., 2006). This is because ENFs in seasonally snow-covered regions undergo a complete downregulation of photosynthesis in winter while remaining continuously green (Adams et al., 2004; Bowling et al., 2018). The utility of reflectance-based indices such as NDVI for detecting phenological events in high-latitude ecosystems is further restricted by rapid transitions, highly variable transition season weather, complex illumination geometry, and the presence of snow cover across the landscape (Maguire et al., 2021; Nelson et al., 2022; Parazoo et al., 2018; Pierrat et al., 2021; Wang et al., 2023).

To overcome the unique set of reflectance-based remote sensing challenges posed by ENFs to be useful for tracking phenology, remote sensing metrics must be sensitive to changes in physiological activity. Metrics used in such tracking efforts must also be able to disentangle the impacts of snow and canopy structure from the physiological signal, which impact vegetation indices across the electromagnetic spectrum (Wang et al., 2023). Solar-induced chlorophyll fluorescence (SIF) has proven to be a powerful metric for determining important phenological events in ENFs due to its mechanistic connection to photosynthetic activity (Cheng et al., 2020, 2022; Magney, Bowling, et al., 2019; Magney, Frankenberg, et al., 2019; Pierrat et al., 2021; Pierrat, Bortnik, et al., 2022; Pierrat, Magney, et al., 2022). SIF is a direct emission from chlorophyll molecules and, therefore, remotely sensed SIF is theoretically less impacted by non-photosynthetic material such as snow and soil than reflectance-based vegetation indices. The biological basis for using SIF to infer changes in plant photochemistry stems from decades of research into the mechanisms of light partitioning at the leaf scale using pulse-amplitude modulation (PAM) fluorescence (Murchie & Lawson, 2013; Pierrat et al., 2024).

After absorption by chlorophyll, light energy can either: (1) drive photochemistry ($\phi_P$); (2) be dissipated as excess energy (non-photochemical quenching, $\phi_N$); (3) be re-emitted as chlorophyll fluorescence ($\phi_F$); or (4) lost as heat through nonradiative transfer of excitation energy ($\phi_D$). These partitioned components account for all absorbed light such that their individual fractional yields

($\phi$) sum to one and changes in one variable lead to compensatory changes in others (Frankenberg & Berry, 2017). Over seasonal time scales and under moderate light conditions, $\phi_P$ and $\phi_F$ tend to vary synchronously, with an opposite change in $\phi_N$ (Porcar-Castell, 2011; Porcar-Castell et al., 2014, 2021); however, the positive covariation between $\phi_P$ and $\phi_F$ can break down under highly stressful conditions (Martini et al., 2022). Due to the general premise that $\phi_P$ and $\phi_F$ covary under conditions relevant to remote sensing measurements (moderate light, Magney et al., 2020), SIF has been widely used as a proxy for canopy photosynthetic activity (Porcar-Castell et al., 2014, 2021; Sun et al., 2017, 2023).

SIF retrieved at the canopy scale can be defined as:

$$\mathrm{SIF} = \mathrm{PAR} \times f\mathrm{PAR}_{\mathrm{chl}} \times \mathrm{LUE}_{\mathrm{F}} \times f_{\mathrm{esc}}, \quad (1)$$

where PAR is the photosynthetically active radiation, $f\mathrm{PAR}_{\mathrm{chl}}$ is the fraction of incident PAR absorbed by chlorophyll, $\mathrm{LUE}_F$ is the light use efficiency of fluorescence (canopy-level $\phi_F$), and $f_{esc}$ is the fraction of emitted SIF photons which escape the canopy to be detected, which is a function of canopy structure and chlorophyll content. Importantly, SIF retrieved at the canopy-scale is a function of chlorophyll content, incident light reaching the canopy, and fluorescence yield.

Canopy-level carbon uptake (GPP) can similarly be defined as:

$$\mathrm{GPP} = \mathrm{PAR} \times f\mathrm{PAR}_{\mathrm{chl}} \times \mathrm{LUE}_{\mathrm{P}}, \quad (2)$$

where $\mathrm{LUE}_P$ is the light use efficiency of photosynthesis (canopy-level $\phi_P$). The relationship between SIF and GPP can thus be described (Guanter et al., 2014):

$$\mathrm{GPP} = \mathrm{SIF} \times \frac{\mathrm{LUE}_{\mathrm{P}}}{\mathrm{LUE}_{\mathrm{F}} \times f_{\mathrm{esc}}}. \quad (3)$$

Based on these equations, SIF and GPP are linked by both shared drivers (PAR × $f\mathrm{PAR}_{\mathrm{chl}}$), as well as biological parameters ($\mathrm{LUE}_P$ and $\mathrm{LUE}_F$). Because evergreen systems do not experience large changes in canopy structure or chlorophyll content seasonally, $f_{esc}$ remains approximately constant (Pierrat, Magney, et al., 2022). Averaged over broad spatiotemporal scales, the $\frac{\mathrm{LUE}_P}{\mathrm{LUE}_F \times f_{esc}}$ term in Equation (3) is approximately constant, making SIF an effective proxy for GPP (Magney, Bowling, et al., 2019; Magney, Frankenberg, et al., 2019; Pierrat, Magney, et al., 2022). However, our interpretation of canopy SIF and the relationships among canopy-scale $\mathrm{LUE}_P$ and $\mathrm{LUE}_F$, and needle-scale $\phi_F$ and $\phi_P$ is challenged by limited comparisons across sites and a lack of coincident needle- and canopy-scale measurements of fluorescence. This is most notable when relating SIF to GPP during the transition seasons.

Recent work has reported an increase in SIF in spring along with increasing PAR prior to changes in GPP in ENFs (Magney, Bowling, et al., 2019; Magney, Frankenberg, et al., 2019; Pierrat, Bortnik, et al., 2022; Pierrat, Magney, et al., 2022; Yang et al., 2022). This raises the question: Is covariation between SIF and GPP merely a result of shared drivers (PAR × $f\mathrm{PAR}_{\mathrm{chl}}$), which decouple during the spring transition when PAR increases but $\mathrm{LUE}_P$ does not, or an actual physiological change in steady-state fluorescence yield? Coupling measurements at multiple scales (leaf and canopy) will help properly disentangle the physiological from the physical SIF signal and answer this question. This will enable further testing of the hypothesis that $\mathrm{LUE}_F$ and $\mathrm{LUE}_P$ co-vary during important phenological transitions due to the co-variation of $\phi_F$ and $\phi_P$. This coupling approach has been used in cropping systems (Kimm et al., 2021), but has yet to be empirically tested in ENFs. We compare canopy-level measurements of SIF, GPP, and derived $\mathrm{LUE}_F$ and $\mathrm{LUE}_P$, with continuous PAM needle-scale fluorescence measurements of $\phi_F$ and $\phi_p$ from research sites in Alaska (Delta Junction, DEJU) and Colorado (Niwot Ridge, US-NR1). We then compare canopy-level estimates of $\mathrm{LUE}_F$ (approximated using intensity-normalized SIF, $\mathrm{SIF}_{\mathrm{relative}}$) and $\mathrm{LUE}_P$ (approximated as GPP/PAR, Equation 2) at DEJU and US-NR1 with a third site in Saskatchewan (Southern Old Black Spruce, Ca-Obs) using multiple years of data. Ultimately, we seek to answer the following two questions:

1. How do the yields of fluorescence and photosynthesis vary across the year in ENFs in cold/winter dormant climates?
2. Considering the unique set of remote sensing challenges posed by snow and persistent greenness in ENFs, how can we best scale fluorescence and photosynthesis measures from the needle to the canopy to capture seasonal transitions?

Answering these questions will help inform the correspondence between needle and canopy-scale measurements related to physiological transitions in ENFs and ultimately improve our ability to monitor ecosystem sensitivity to environmental change.

# METHODS

## Study sites

We collected data at three ENF locations: Niwot Ridge AmeriFlux core site US-NR1, Southern Old Black Spruce

site Ca-Obs, and NEON Delta Junction, DEJU. These three sites are ideal candidates for this study because they (1) exhibit strong seasonality in photosynthesis driven by sub-zero temperatures in winter; (2) experience seasonal snow cover which complicates the use of reflectance-based metrics for determining photosynthetic seasonality and; (3) are at a broad range of latitudes and therefore experience large differences in the seasonality of available light (PAR). The site locations, average meteorological conditions, and vegetation are summarized in Table 1.

At DEJU and US-NR1, continuous PAM fluorescence, eddy covariance, and tower-based remote sensing data were collected (Figure 1). At Ca-Obs, only tower remote sensing and eddy covariance data were collected. Meteorological data including air temperature, PAR, and others not presented in this study were collected at all sites.

## Needle-scale fluorescence measurements

Continuous PAM fluorescence data were collected using a MONI-PAM fluorometer (Walz GmBH, Germany) at both DEJU and US-NR1. The MONI-PAM is an active fluorometer system that uses weak modulated light to continuously measure fluorescence emission from needles with preprogramed saturating pulses (every 2 h) to obtain steady-state fluorescence ($F_o$ at night and $F_t$ during the day) and maximal fluorescence emission ($F_m$ at night and $F_m'$ during the day, see Maxwell & Johnson, 2000 for notation). The US-NR1 MONI-PAM was installed on March 15, 2018, and ran until August 30, 2018. The DEJU MONI-PAM was installed on August 18, 2021, and ran through August 15, 2022. At US-NR1, one sensor head was installed on a south-facing lodgepole pine branch to avoid shadowing effects approximately 5 m off the ground via a canopy access tower. Ten lodgepole pine needles were placed on a plane within the leaf clip similar to Kim et al. (2021) and Porcar-Castell (2011). At DEJU, four sensor heads were installed at roughly 2 m off the ground on individual black spruce branches of four separate trees. Each sensor head was oriented in a different direction to ensure that at least one sensor head was in direct sunlight at any given time. PAM fluorescence data is sensitive to incident illumination conditions; however, because the MONI-PAM data is averaged across all sensors and over the entire day (i.e., at any given time one might be sunlit while the others are in the shade). These data thus provide accurate daily baseline conditions associated with fluorescence and photochemical yields.

**TABLE 1** General overview of sites where data were collected for this study.

| Site | US-NR1 (Colorado) | Ca-Obs (Saskatchewan) | DEJU (Alaska) |
|---|---|---|---|
| Lat/lon | 40.03° N, 105.55° W | 53.98° N, 105.12° W | 63.88° N, 145.75° W |
| Elevation | 3050 m | 629 m | 517 m |
| Mean annual air temp | 2.8°C | 1.4°C | 0.4°C |
| Mean annual precipitation | 800 mm | 428 mm | 305 mm |
| No. days annually with snow depth >1 cm | ~200–230 days | ~130–160 days | ~220–250 days |
| Canopy height | 13 m | 16 m | 10 m |
| Overstory vegetation | Lodgepole pine (*Pinus contorta*), Englemann spruce (*Pinus engelmannii*), and subalpine fir (*Abies lasiocarpa*) | Predominantly (90% stem density) black spruce (*Picea mariana*) and scattered (10%) larch (*Larix laricina*) | Black and white spruce (*Picea mariana* and *Picea glauca*) |
| Understory vegetation | Sparsely vegetated (~25% average understory coverage) with *Vaccinium myrtillus* | Mixed feather mosses (*Hylocomium splendens, Pleurozium schreberi, Ptilium cristacastrensis*) with some peat moss (*Sphagnum* spp.) and lichen (*Cladina* spp.) | Sedges, mosses, and low-growing shrubs including lingonberry (*Vaccinium vitis-idaea*), crowberry (*Empetrum nigrum*), bog blueberry (*Vaccinium uliginosum*), bog Labrador tea (*Ledum palustre*), false toadflax (*Geocaulon lividum*), and bearberry (*Arctostaphylos uva-ursi*) |
| Sources | Burns et al. (2015), Monson et al. (2010) | Chen et al. (2006), Jarvis et al. (1997) | Delta Junction NEON\|NSF NEON (n.d.) |

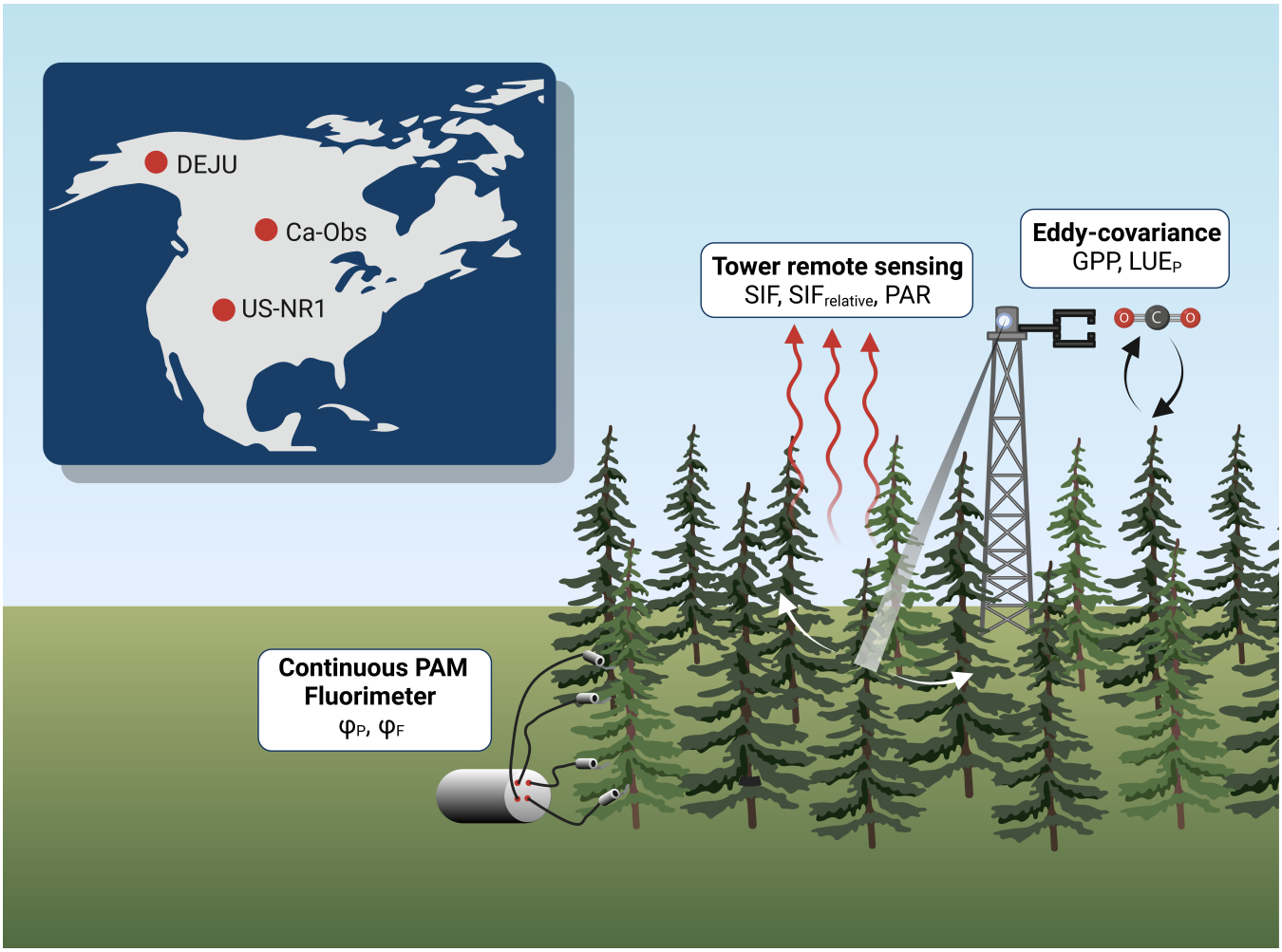


**FIGURE 1** General overview of measurements and parameters derived from instruments at the study sites. Note that Ca-Obs did not have continuous PAM fluorometer data available. An inset map shows the location of each study site. Created with BioRender.com. GPP, gross primary productivity; $LUE_P$, light use efficiency of photosynthesis; PAR, photosynthetically active radiation; SIF, solar-induced chlorophyll fluorescence.

Given that black spruce needles are too short to create a "flat-mat" of needles (Kim et al., 2021; Porcar-Castell, 2011), we did not manually manipulate the needles and instead placed a stem of ~25 needles in the field of view (FOV) of the MONI-PAM. At both sites, the sensor heads were programed to deliver a 0.8-s saturating pulse every 2 h. Saturating light intensity (sensor setting 11) was chosen to ensure a rectangular saturating maximal fluorescence emission response. The MONI-PAM detects >87% of light at wavelengths greater than 660 nm (Heinz Walz GmbH, 2023). From the MONI-PAM data, we report steady-state fluorescence yield ($\phi_F$) and photochemical yield ($\phi_P$), averaged across all four instruments. $\phi_F$ is computed as $0.1 \times (F_t/F_{mR})$, where $F_{mR}$ is a summer night reference measured in the absence of sustained non-photochemical quenching (NPQ) (Kim et al., 2021; Zhang et al., 2019). The $F_{mR}$ value here assumes a maximum fluorescence yield of 10% for PSII under a saturating pulse ($F_m$), and combines the total yield of fluorescence and basal thermal energy dissipation—which has been widely adapted to provide information on the seasonal dynamics of $\phi_F$ (Barber et al., 1997; Kim et al., 2021; Porcar-Castell, 2011; Zhang et al., 2019). $\phi_P$ is computed as $(F_m' - F_t)/F_m'$, where $F_m'$ is maximal fluorescence under light and $F_t$ is steady-state fluorescence during the day (Porcar-Castell, 2011).

## Tower-based remote sensing measurements

We collected remotely-sensed measurements of vegetation reflectance (400–950 nm) and far-red SIF using a custom spectrometer (PhotoSpec Grossmann et al., 2018) at each forest. SIF was retrieved in the far-red

(745–758 nm) wavelength range using a Fraunhofer-line-based fitting algorithm (Grossmann et al., 2018). Fraunhofer-lines are dark spectral lines inherent in the solar spectrum itself and caused by elemental absorption in the Sun's atmosphere (Figure 2b). Because SIF is an emitted signal, it provides an additive offset, which reduces the optical depth of these well-known spectral features (Grossmann et al., 2018). The change in optical depth is used to retrieve the SIF signal. The wavelength region used for our retrieval was additionally selected to exclude absorption features from water and oxygen to improve retrieval stability under variable atmospheric conditions. The Fraunhofer-line-based approach makes SIF retrievals insensitive to atmospheric scattering and therefore robust even under cloudy sky conditions (Chang et al., 2020; Frankenberg & Berry, 2017; Mohammed et al., 2019).

PhotoSpec was installed in all three sites at the top of the scaffolding/eddy-covariance tower facing due north. It has a narrow FOV (0.7°), 2-D scanning capabilities, and takes a measurement approximately every 30 s (Grossmann et al., 2018). We took canopy representative scans within a 30 min window at all field locations and removed low-quality data with high retrieval uncertainties or unstable illumination conditions during the measurement window (Grossmann et al., 2018; Magney, Bowling, et al., 2019; Magney, Frankenberg, et al., 2019; Pierrat et al., 2021; Pierrat, Magney, et al., 2022). In addition to SIF, we calculated $SIF_{relative}$ for each measurement following Equation (4) and averaged canopy scans together to report half-hourly data for SIF and $SIF_{relative}$.

Because SIF is sensitive to both $LUE_F$ and $APAR_{chl}$ ($APAR_{chl} = PAR \times fPAR_{chl}$) (Equation 1), the spring onset of photosynthesis can be difficult to decipher from changes in $APAR_{chl}$ when using SIF directly (Magney, Bowling, et al., 2019; Magney, Frankenberg, et al., 2019; Pierrat, Magney, et al., 2022; Yang et al., 2022). To test the covariation between $LUE_F$ and $LUE_P$ we need to separate the physical ($f_{esc}$, $APAR_{chl}$) from the physiological ($LUE_F$) influences on the SIF signal.

Our approach for separating the physiological from the physical SIF signal is to estimate $LUE_F$ using $SIF_{relative}$ (Butterfield et al., 2023; Cheng et al., 2020; Parazoo et al., 2020; Pierrat et al., 2021). $SIF_{relative}$ is the ratio of emitted SIF per reflected radiance ($I$) in the portion of the spectrum where SIF retrievals occur (Figure 2b) as:

$$SIF_{relative} = \frac{SIF(\lambda)}{I(\lambda)}, \quad (4)$$

where ($\lambda$) indicates the wavelength region of interest (in our case far-red 745–758 nm). This normalization is useful because it corrects the SIF signal for canopy radiative transfer effects to get at $LUE_F$ as demonstrated below. We can say that the radiance measured at the detector, $I(\lambda)$, is:

$$I(\lambda) = I(\lambda)_{leaf} \times f_{esc}(\lambda), \quad (5)$$

where $I(\lambda)_{leaf}$ is the radiance emitted at the leaf level and $f_{esc}(\lambda)$ is the fraction of photons escaping the canopy in that wavelength range. Because SIF($\lambda$) and $I(\lambda)$ have the same $f_{esc}(\lambda)$, we can combine Equations (1) and (5) to solve for $LUE_F$:

$$LUE_F = \frac{SIF(\lambda) \times I(\lambda)_{leaf}}{I(\lambda) \times APAR_{chl}}. \quad (6)$$

Although chlorophyll absorption in the 400–700 nm PAR range leads to a wavelength-dependence on the relationship between $I(\lambda)_{leaf}$ and $APAR_{chl}$ (Guidi et al., 2017), overall canopy radiative transfer is dominated by shadowing effects which do not have strong wavelength dependence. Thus, the wavelength dependence is small compared with the variability from shadowing, and we can say that $I(\lambda)_{leaf}$ and $APAR_{chl}$ are proportional for a given viewing direction. We can then eliminate $I(\lambda)_{leaf}$ and $APAR_{chl}$ in Equation (5) to arrive back at:

$$LUE_F \approx SIF_{relative} = \frac{SIF(\lambda)}{I(\lambda)}. \quad (7)$$

While a variety of corrections have been proposed to isolate the physiological response of SIF ($LUE_F$) by correcting for the physical effects ($f_{esc}$ and $APAR_{chl}$) (Dechant et al., 2020; Yang et al., 2020; Zeng et al., 2019, 2020), we compute $SIF_{relative}$ because it does not rely on vegetation indices (which are shown to be highly impacted by snow cover, as shown in *Accounting for snow impacts on SIF retrievals*). Furthermore, it does not require additional measurements (of $APAR_{chl}$ or other) which can be highly uncertain or introduce additional sources of error. Finally, because SIF($\lambda$) and $I(\lambda)$ have the same radiometric calibration, this approach also corrects for calibration uncertainty and deterioration over time.

One complicating factor in this argument is the presence of snow, which is often present during the spring transition. Because we aim to capture spring and fall dynamics even when snow is present, we cannot exclude observations under snow-covered conditions and, therefore, must consider the impact of snow onto SIF and $SIF_{relative}$ in more detail. Snow cover is intermittently present in the canopy during spring transition, and because of the rapid onset of photosynthetic activity and SIF dynamics during this compressed period, it is

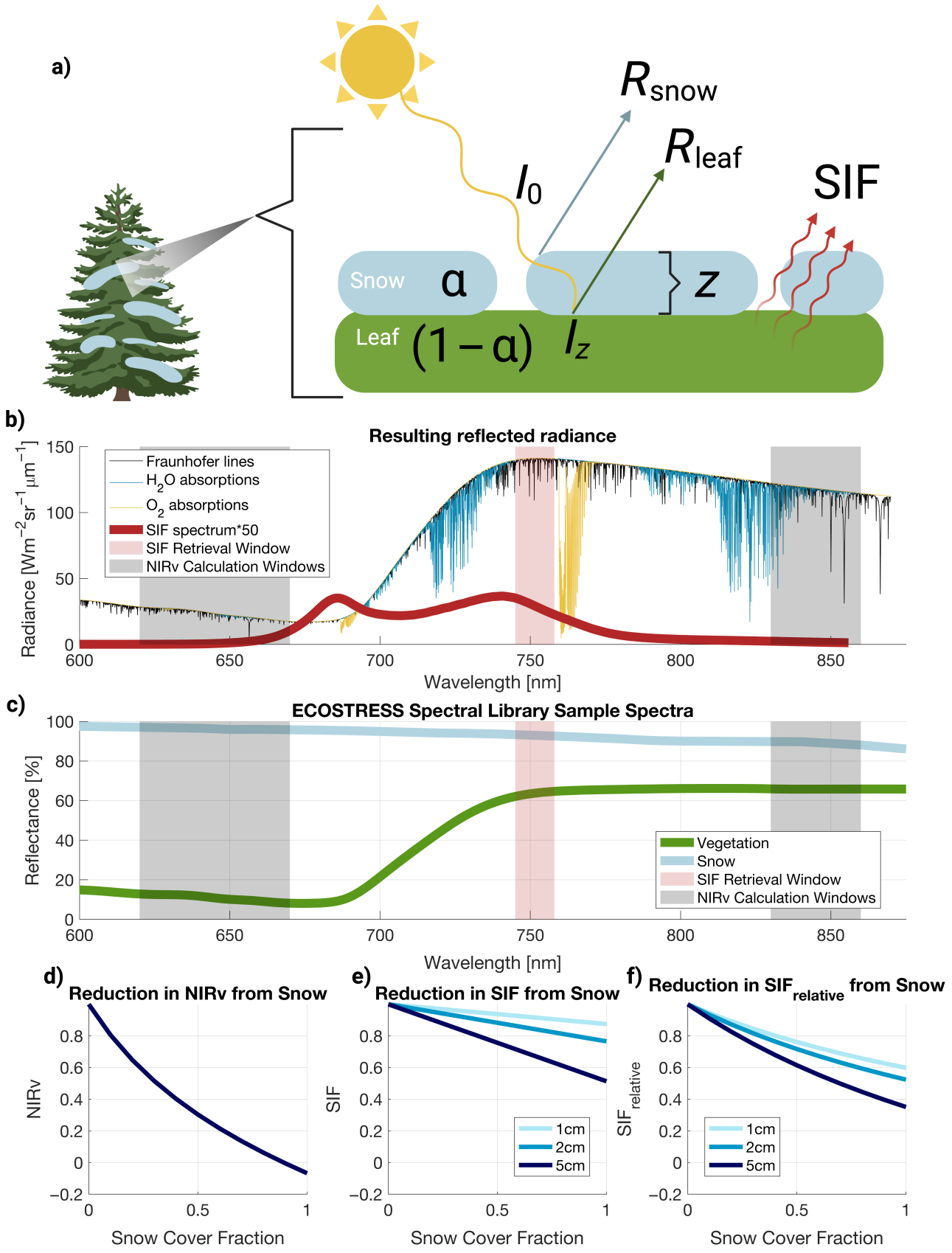


**FIGURE 2** Legend on next page.

necessary to retain observations for comprehensive examination rather than exclude due to snow contamination.

## Accounting for snow impacts on SIF retrievals and reflectance

Photosynthesis can begin under snow if temperatures are warm enough and light is able to penetrate the snow (Starr & Oberbauer, 2003). Therefore, we cannot simply eliminate data with potential snow contamination. We justify not filtering for snow based on the following conceptual comparison of the impacts of snow on SIF, $SIF_{relative}$, and a common reflectance index used to correct for illumination effects on SIF, the near-infrared vegetation index (NIRv; Badgley et al., 2017). NIRv is normalized difference vegetation index (NDVI) multiplied by reflected radiation in the NIR. This metric has gained recent popularity in tracking photosynthesis across a variety of ecosystems and has been used to correct SIF for illumination effects (Badgley et al., 2019; Dechant et al., 2020; Zeng et al., 2019). We illustrate this with the following idealized calculation to understand the impacts of snow on SIF, $SIF_{relative}$, and NIRv.

The intensity of retrieved light at a particular wavelength ($I$) can be defined as the product of incoming light at a particular wavelength ($I_0$) and reflectance ($R$). If we assume the instrument FOV contains a mixture of exposed leaf and snow cover, we can set a fraction of snow in the instrument FOV as α (Figure 2a). Thus, the intensity of the retrieved light at a particular wavelength will be a combination of the reflectance from both snow ($R_{snow}$) and leaf ($R_{leaf}$) at that wavelength as:

$$I = I_0 \times R = I_0(\alpha R_{snow} + (1-\alpha)R_{leaf}). \quad (8)$$

We can use this to determine the dependence of NIRv on the fraction of snow cover in the instrument FOV. NIRv is calculated as:

$$NIRv = \frac{R_{NIR} - R_R}{R_{NIR} + R_R} \times R_{NIR}, \quad (9)$$

where $R_{NIR}$ is the reflectance in the near-infrared (840–876 nm), $R_R$ is the red reflectance (620–670 nm). By substituting Equation (8) into Equation (9), we derive the following equation for the dependence of NIRv on snow fraction.

$$NIRv = \frac{\alpha R_{snowNIR} + (1-\alpha)R_{leafNIR} - \alpha R_{snowR} - (1-\alpha)R_{leafR}}{\alpha R_{snowNIR} + (1-\alpha)R_{leafNIR} + \alpha R_{snowR} + (1-\alpha)R_{leafR}} \times \alpha R_{snowNIR} + (1-\alpha)R_{leafNIR} \quad (10)$$

We tested this equation for the sensitivity of NIRv at a constant intensity using sample reflectance spectra of both pure vegetation and snow from the ASTER spectral library (Baldridge et al., 2009) shown in Figure 2c. The normalized results of this test for NIRv are shown in Figure 2c. Here, we can see that NIRv is highly sensitive to the presence of snow cover and can even become negative in the case of a fully snow-covered pixel (Figure 2d). This is due to the spectral differences between snow (highly reflective) and vegetation spectra (highly absorptive) in the red 620–670 nm wavelength range (Figure 2c).

In contrast to NIRv, which depends on reflected radiance, SIF is an emitted signal. The measured SIF signal is composed of:

$$SIF = SIF_{directly\ from\ leaf} + SIF_{emitted\ through\ snow}. \quad (11)$$

Since SIF depends on the incoming light (Equation 1), we must consider the radiative transfer of light both into and out of the snow overlying vegetation cover. Light traveling through a snowpack depth $z$ and an e-folding length $\varepsilon$ can be defined as:

$$I_z = I_0 e^{-(z/\varepsilon)}. \quad (12)$$

$SIF_{emitted\ through\ snow}$ will be the product of $SIF_{directly\ from\ leaf}$ and the decrease over distance of the snowpack such that:

$$SIF = SIF_{directly\ from\ leaf} + SIF_{emitted\ under\ snow} \times e^{-(z/\varepsilon)}. \quad (13)$$

The emitted SIF signal at the leaf level depends on APAR, $LUE_F$, and $f_{esc}$ (Equation 1). For this test case, we

**FIGURE 2** (a) Assumptions of a "mixed pixel" within a PhotoSpec retrieval, composed of both snow and leaf contributions, used in Equations (8–15). (b) Simulated contributions to reflected radiance measured by PhotoSpec by combining simulated canopy reflectance and solar irradiance. Also shown is an amplified example solar-induced chlorophyll fluorescence (SIF) spectrum and shaded regions where SIF is retrieved and near-infrared vegetation index (NIRv) is calculated. Adapted from Frankenberg and Berry (2017). (c) Example spectra taken from the ECOSTRESS Spectral Library of vegetation and snow, with bars indicating the retrieval windows for both SIF and NIRv. (d–f) Sensitivity tests of the reduction in signal at 1, 2, and 5 cm depths for NIRv (d), SIF (e), and $SIF_{relative}$ (f). Created with BioRender.com.

assume that at a single moment in time $LUE_F$ and $f_{esc}$ are constant and that APAR is proportional to the incident radiation at the leaf ($I_0$). Thus, the SIF signal emitted from non-snow-covered surfaces will be proportional to the incident radiation over non-snow-covered surfaces ($SIF_{directly\ from\ leaf} \propto I_0(1-\alpha)$) and the SIF signal emitted from snow-covered surfaces will be proportional to the incident radiation traveling through snow ($SIF_{emitted\ under\ snow} \propto I_0 \times \alpha \times e^{-(z/\varepsilon)}$). Combining this conceptual framework with Equation (10) we can say that:

$$SIF = I_0(1-\alpha) + I_0 \times \alpha \times e^{-(2z/\varepsilon)}. \quad (14)$$

We tested the dependence of SIF at a constant normalized intensity to the fraction of snow cover at a variety of potential snow depths, assuming an e-folding depth of light in the SIF retrieval window (745–758 nm) of $\varepsilon = 15$ cm (Figure 2e; Galbavy et al., 2007).

$SIF_{relative}$ is the SIF signal divided by the intensity of the light in the retrieval window (Equation 4); therefore, we can define the sensitivity of $SIF_{relative}$ to snow cover fraction by substituting Equations (8) and (14) into Equation (4) so that:

$$SIF_{relative} = \frac{1-\alpha+\alpha \times e^{-(2z/\varepsilon)}}{\alpha R_{snow} + (1-\alpha)R_{leaf}}. \quad (15)$$

We tested this normalized equation and show the dependence of $SIF_{relative}$ on snow cover fraction for a variety of snow depths and an e-folding depth of $\varepsilon = 15$ cm (Figure 2f).

This example shows that both SIF and $SIF_{relative}$ signals depend on snow cover fraction due to the loss of light traveling through the snowpack, however, the sensitivity of these signals is significantly less than the sensitivity of reflectance-based metrics due to the emitted nature of the SIF signal. Therefore, we retain SIF values presented in the manuscript under snow conditions, as the onset of photosynthesis can often begin prior to snow melt in these systems (Pierrat et al., 2021; Starr & Oberbauer, 2003).

## Ecosystem fluxes

GPP was partitioned from estimates of Net Ecosystem Exchange (NEE) using the eddy covariance method. Details on the partitioning can be found in Pierrat, Bortnik, et al. (2022) for DEJU and Ca-Obs and Magney, Bowling, et al. (2019) and Magney, Frankenberg, et al. (2019) for US-NR1. At Ca-Obs, measurements were taken using a 3D sonic anemometer (CSAT3, Campbell Scientific, Logan, UT) in combination with a closed-path infrared gas ($CO_2/H_2O$) analyzer (LI-7200 analyzer, Li-COR, Lincoln, NE) operated in absolute mode. We performed quality assurance on the data using the standard Fluxnet-Canada method following (Barr et al., 2004, 2006). For DEJU, data were obtained from (National Ecological Observatory Network [NEON], 2022) using a Campbell Scientific CSAT-3 3D Sonic Anemometer and LI-COR—LI7200 gas analyzer. We performed quality assurance on carbon fluxes based on turbulent and storage fluxes separately, using a bivariate statistical procedure for each, to overcome quality flag restrictions in the "expanded" NEON eddy-covariance bundle. The 3% outliers (3% of rarest events from the tails of each distribution) were excluded from joint probability distributions for all available data for (a) turbulent flux and PAR, and separately for (b) storage flux and time of day. Net Ecosystem Exchange (NEE) data were considered valid if both the turbulent and storage fluxes passed this quality control step (and NEE is equal to their sum). At US-NR1, the vertical exchange of $CO_2$, including storage, was measured at a height of 21.5 m by eddy covariance using a sonic anemometer (model CSAT3; Campbell Scientific) coupled with a closed-path infrared gas analyzer (model LI-6262; LI-COR Biosciences)—details are available in Burns et al. (2015). At all sites, data for NEE and meteorological variables were filtered to remove low turbulence (low-friction velocity) periods, and then gap-filled via the R package REddyProc (Wutzler et al., 2018). REddyProc was used to partition NEE into GPP and total ecosystem respiration, $R_{eco}$ with air temperature used as the driving temperature for $R_{eco}$ (Lasslop et al., 2010).

We calculated a canopy approximation for $LUE_P$ using Equation (2). We assume $fPAR = 1$ and is constant through the course of the season, and therefore $LUE_P = GPP/PAR$ (Barton & North, 2001; Nichol et al., 2000; Suyker et al., 2004). Although $fPAR$ is not equal to 1, this would only change the $LUE_P$ values by a constant scaling factor and therefore is irrelevant for evaluating the timing of the spring and fall transitions. NDVI and NIRv values during the growing season show minimal changes further supporting the idea that $fPAR$ is approximately constant (Appendix S1: Figure S1). Finally, we forced all $LUE_P$ values calculated with either a GPP value $<1\ \mu mol\ m^2\ s^{-1}$ or a PAR value $<1\ \mu mol\ m^2\ s^{-1}$ to be zero as the division by such a small number led to significant scatter in our data, and it is a reasonable assumption that negligible photosynthesis is happening under extremely low light conditions.

# RESULTS AND DISCUSSION

## Needle-level fluorescence and photosynthesis yields

MONI-PAM data from both US-NR1 and DEJU show seasonal co-variation between the yields of fluorescence ($\phi_F$) and photochemistry ($\phi_P$) (Figure 3). Between the spring and fall, both $\phi_F$ and $\phi_P$ increase and decrease in synchrony—with some variation throughout the summer (Figure 3a,c). In spring at DEJU, the increase in $\phi_F$ and $\phi_P$ occurs while air temperatures are consistently above zero, but snow is still present. At US-NR1 snow cover is more variable and an increase in $\phi_F$ and $\phi_P$ occurs during warm spells, followed by occasional snow events (similar to Pierrat et al., 2021). Given that photochemistry activates while snow is still present, any remotely sensed proxy for photosynthetic phenology must be sensitive to both underlying leaf level biology and relatively robust against the presence of snow (i.e., Figure 2).

Importantly, both $\phi_F$ and $\phi_P$ remain above zero for most of the winter at both sites (Figure 3a,c). This supports previous findings that despite reduced antenna size and the development of sustained nonphotochemical quenching, there is only a partial loss of photosystem II, which remains intact during the winter to dissipate absorbed energy as heat through charge separation and recombination (Öquist & Huner, 2003). This results in a small emission of steady-state fluorescence during the winter (Bowling et al., 2018; Porcar-Castell, 2011), which can be detected using remote sensing techniques (*Seasonal trends in canopy-scale SIF and GPP*). Over the entire dataset, $\phi_F$ and $\phi_P$ are highly correlated with $r^2 = 0.74$ and 0.70 at US-NR1 and DEJU, respectively (Figure 3b,d). Interestingly the relationship between $\phi_F$ and $\phi_P$ tends to show some seasonal hysteresis at both DEJU and US-NR1. In the spring, $\phi_F$ and $\phi_P$ increase in parallel, and in the fall, a more rapid decrease in $\phi_F$ than in $\phi_P$ is observed. This suggests that maximal fluorescence emission under a saturation pulse ($F_m'$) might be changing less than minimal steady-state fluorescence emission ($F_t$). Winter depression in both $F_t$ and $F_m$ can be the result of a reduction in D1 PSII reaction center proteins (Ensminger et al., 2001; Ottander et al., 1995) and the presence of sustained NPQ—leading to downregulation of the reaction centers (Porcar-Castell, 2011; Porcar-Castell et al., 2008) and potentially a faster relative response in $F_t$ than $F_m'$. This could suggest decoupling between fluorescence and photochemical yields in the fall, and more work along these lines is needed.

The strong positive relationship between $\phi_F$ and $\phi_P$ provides support for the hypothesis that over seasonal

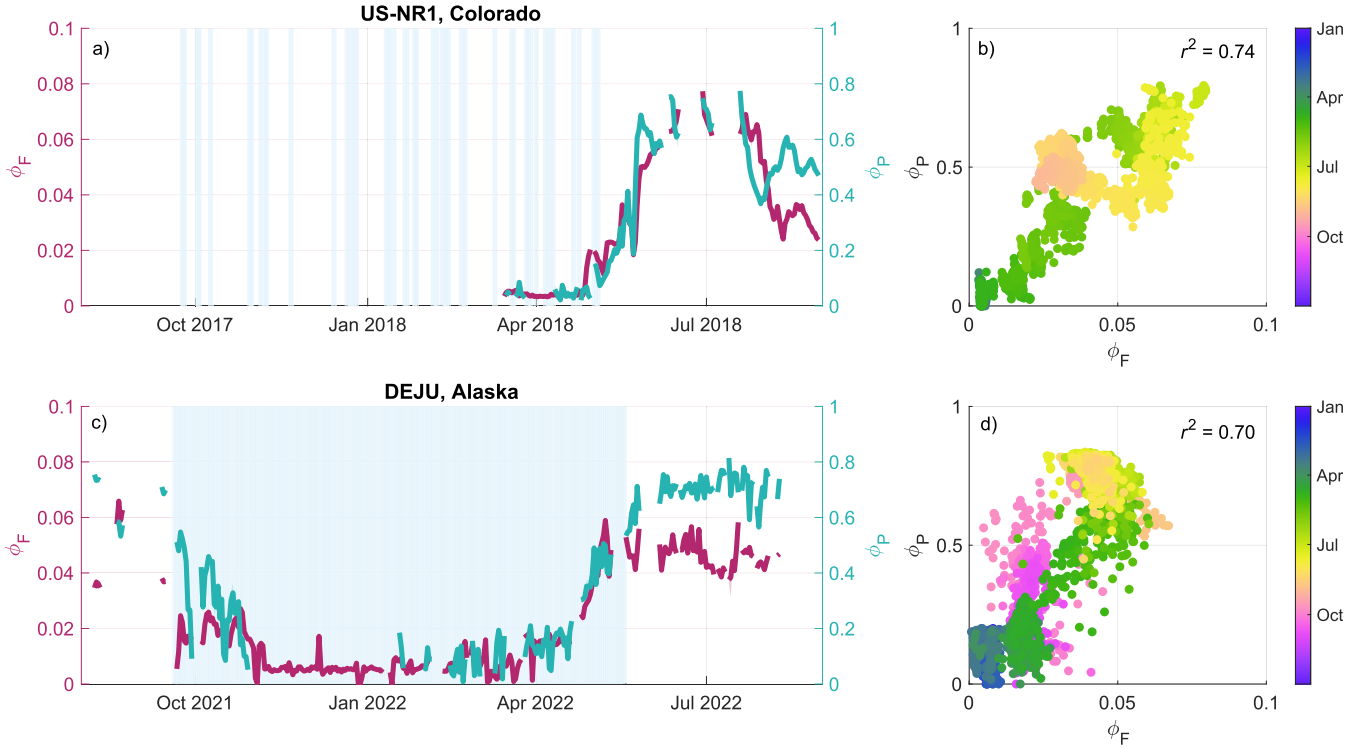


**FIGURE 3** Daily averages of needle-scale fluorescence ($\phi_F$) and photochemical ($\phi_P$) yield data for US-NR1 (a) and DEJU (c) from MONI-PAM. Vertical light blue bars indicate snow presence on the canopy, as observed from tower webcams. Scatterplots of daily average $\phi_F$ and $\phi_P$ at US-NR1 (b) and DEJU (d) over the course of the sampling period, colored by month.

time scales, $\phi_F$ and $\phi_P$ tend to covary. However, when $\phi_F$ and $\phi_P$ are observed over shorter time scales (diurnally) and under low light conditions, a negative relationship between $\phi_F$ and $\phi_P$ has been observed in evergreen forests (Maguire et al., 2020). Additionally, under high light and high stress conditions, there has been evidence of decreases in $\phi_P$ with an increase in $\phi_F$ (Martini et al., 2022). Martini et al. (2022) observed this phenomenon during a heatwave in a Mediterranean forest and explain this as a saturation of NPQ, causing a change in the allocation of energy dissipation pathways toward $\phi_F$. It is also worth noting that even with correspondence between $\phi_F$ and $\phi_P$, as is observed in our data, changes in photochemistry do not necessitate a change in gas-exchange (Maguire et al., 2020). In boreal conifers, photosynthetic gas exchange decreases rapidly in response to freezing temperatures, and will cease when water freezes extracellularly (Kolari et al., 2007; Nehemy et al., 2023; Öquist, 1983). Differences in $\phi_P$ and net photosynthesis are often observed in the springtime in overwintering evergreen systems, as the light harvesting reactions of photosystem II are relatively temperature insensitive while the Calvin cycle reactions are more temperature sensitive (Sevanto et al., 2006). At the same time, observations of strong downregulation of PSII have been found during the fall transition in boreal conifers, often in synchrony with decreases in photosynthetic gas exchange (Ensminger et al., 2004; Lundmark et al., 1998). While our data suggest potential coordination between light (photochemistry) and carbon reactions (photosynthesis), we are limited by a lack of needle-scale gas-exchange measurements—but we can test this hypothesis using tower-based eddy covariance and remote sensing data (*Seasonal trends in canopy-scale SIF and GPP*).

## Seasonal trends in canopy-scale SIF and GPP

Daily changes in both GPP and SIF, as well as $SIF_{relative}$ (as a proxy for $LUE_F$) and $LUE_P$, illustrate the coordination of fluorescence and photochemical/photosynthetic activity at the canopy scale. The seasonal trends in SIF and GPP (Figure 4) are consistent with prior observations of daily tower-based SIF and GPP in ENFs (Magney, Bowling, et al., 2019; Magney, Frankenberg, et al., 2019; Pierrat, Bortnik, et al., 2022; Pierrat, Magney, et al., 2022; Yang et al., 2022). Across all three sites, GPP shows a winter dormant period and a summer photosynthetic period, whereby GPP increases in spring when air temperature is above 0°C, but prior to the disappearance of snow (Figure 4). GPP then remains elevated until the first snowfall or later (Figure 4). The seasonal cycle of SIF shows good agreement with the seasonal cycle of GPP with a winter dormancy and summer growing season (Figure 4a–c). While GPP goes to zero in the winter, there

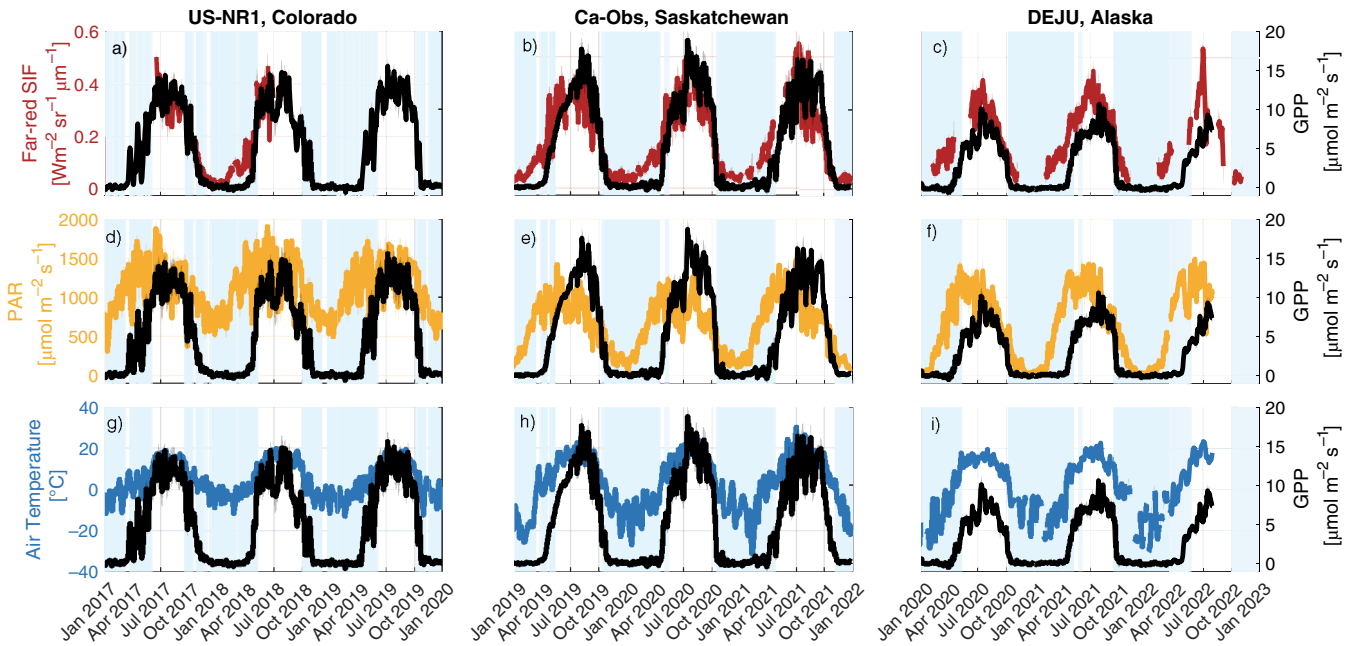


**FIGURE 4** Time series of five-day moving average gross primary productivity (GPP) (black) and far-red solar-induced chlorophyll fluorescence (SIF) (red) for US-NR1 (a), Ca-Obs (b), and DEJU (c). Time series of five-day moving average GPP (black) and photosynthetically active radiation (PAR) (gold) for US-NR1 (d), Ca-Obs (e), and DEJU (f). Time series of five-day moving average GPP (black) and air temperature (blue) for US-NR1 (g), Ca-Obs (h), and DEJU (i). Vertical blue lines indicate snow on the canopy.

is still a small amount of fluorescence emission (SIF > 0). Across all three tower sites, SIF increases prior to GPP in spring, but generally follows GPP in the fall. In contrast, vegetation indices sensitive to greenness (NDVI and NIRv) tend to show little seasonality at these sites because ENFs retain chlorophyll year-round and there is little change in canopy structure (Appendix S1: Figure S1; Magney, Bowling, et al., 2019; Magney, Frankenberg, et al., 2019; Pierrat, Magney, et al., 2022; Pierrat, Bortnik, et al., 2022; Pierrat et al., 2024). The seasonality observed from our greenness-based vegetation index data (NDVI and NIRv; Appendix S1: Figure S1) is due to changes in snow cover and/or emergence of canopy understory within the instrument FOV (Sims et al., 2006; Wang et al., 2023). Wang et al. (2023) showed dramatic changes across the electromagnetic spectrum due to snow (based on ground measurements), which corroborates our test case (Figure 2), providing further evidence that snow sensitivity will impact interpretation of the seasonal timing of photochemistry in ENFs from reflectance-based remote sensing platforms.

The spring increase in SIF (Figure 4) prior to the onset of GPP can be attributed to a persistent SIF light response over winter (Appendix S1: Figure S1; also reported in Pierrat, Magney, et al., 2022; Pierrat, Bortnik, et al., 2022; Yang et al., 2022). Over the winter months (e.g., January–March, November, December) water limitations from frozen boles and small stems (Nehemy et al., 2023; Sevanto et al., 2006) and sustained NPQ (Adams et al., 2004; Bowling et al., 2018; Verhoeven, 2014) inhibit photosynthesis. This abolishes the GPP light response across all three sites (Appendix S1: Figure S2). In contrast, SIF over winter has a small, but non-zero, response to light (Appendix S1: Figure S2). This is supported by our measurements of non-zero $\phi_F$ during winter at the needle scale (Figure 3; Ottander et al., 1995; Porcar-Castell, 2011; Walter-McNeill et al., 2021). To clarify the relationship between SIF and GPP, particularly during the transition months, we must develop techniques to disentangle the impact of PAR on remote sensing signals (i.e., SIF) to represent $LUE_F$ in a way that can capture the spring transition in seasonally snow-dominated ecosystems. Because SIF and $SIF_{relative}$ are less impacted by the presence of snow (Figure 2), we assess the effectiveness of $SIF_{relative}$ for tracking phenological events at the canopy scale (*Coordination of fluorescence and photosynthetic yields across spatial scales*).

## Coordination of fluorescence and photosynthetic yields across spatial scales

To explore how needle-scale dynamics between $\phi_F$ and $\phi_P$ scale to the canopy level, we compared $\phi_F$ and $\phi_P$ with their canopy-level proxies, $SIF_{relative}$ and $LUE_P$ (Figures 5 and 6). Seasonally, $LUE_P$ and $\phi_P$ tend to covary in the timing of both spring onset and fall cessation (Figure 5a,c). However, $LUE_P$ and $\phi_P$ show a weak-moderate correlation seasonally across both sites ($r^2 = 0.25$ and $r^2 = 0.61$ at US-NR1 and DEJU respectively, Figure 5b,d). The shape of the relationship between $LUE_P$ and $\phi_P$ is also notably different between US-NR1 and DEJU, where a saturation is observed at high $\phi_P$ values at DEJU. While these relationships tend to covary positively, the weak-moderate correlation between $LUE_P$ and $\phi_P$ can likely be attributed to the fact that $LUE_P$ is highly variable during the growing season. Because $LUE_P$ tends to decrease under high light (Figure 7), rapidly fluctuating light conditions during the growing season can explain the variability in $LUE_P$. Additionally, $LUE_P$ values calculated in winter can be noisy when PAR is near zero due to the division of GPP by PAR (this is most notable at DEJU). Given that our $\phi_P$ measurements were daily averages from lower branches in the canopy, and were exposed to more consistent illumination conditions, the seasonal trajectory of $\phi_P$ is more smooth than $LUE_P$.

At both sites, we observe synchronous timing of $\phi_P$ and $LUE_P$ before the snow has melted, suggesting coordination between photochemistry at the needle scale and estimates of canopy photosynthesis. In particular, there was a small increase in both $\phi_P$ and $LUE_P$ in April 2018 at US-NR1, prior to a sub-zero air temperature and snow event. Photochemical efficiency ($\phi_P$) and canopy photosynthetic efficiency ($LUE_P$) tend to covary early in the spring, prior to the summer growing season. This is consistent with observations at Ca-Obs, which showed that during the spring transition period, the timing of photochemical activity via fluorescence emission ($SIF_{relative}$) covaried with transpiration-induced water transport and GPP (Pierrat et al., 2021). In support of this, Springer et al. (2017) observed parallel seasonal patterns of photosynthesis and fluorescence measurements during the spring and fall transitions in a boreal forest using bi-weekly needle-scale measurements. Given these multiple lines of evidence, we can conclude that a coordination between both the light and carbon reactions exists during transition periods.

To explore the relationship between $\phi_F$ and $LUE_F$, we tested the use of $SIF_{relative}$ as a proxy for $LUE_F$ (Figure 6). At both US-NR1 and DEJU, $SIF_{relative}$ showed good correlation with $\phi_F$ ($r^2 = 0.65$ and 0.61 respectively), and good agreement on the timing of seasonal increases and decreases in $\phi_F$ (Figure 6). Unfortunately, there was a data gap in $SIF_{relative}$ during the spring transition at DEJU which limits our ability to directly relate the timing of increasing $SIF_{relative}$ and $\phi_F$ during the spring

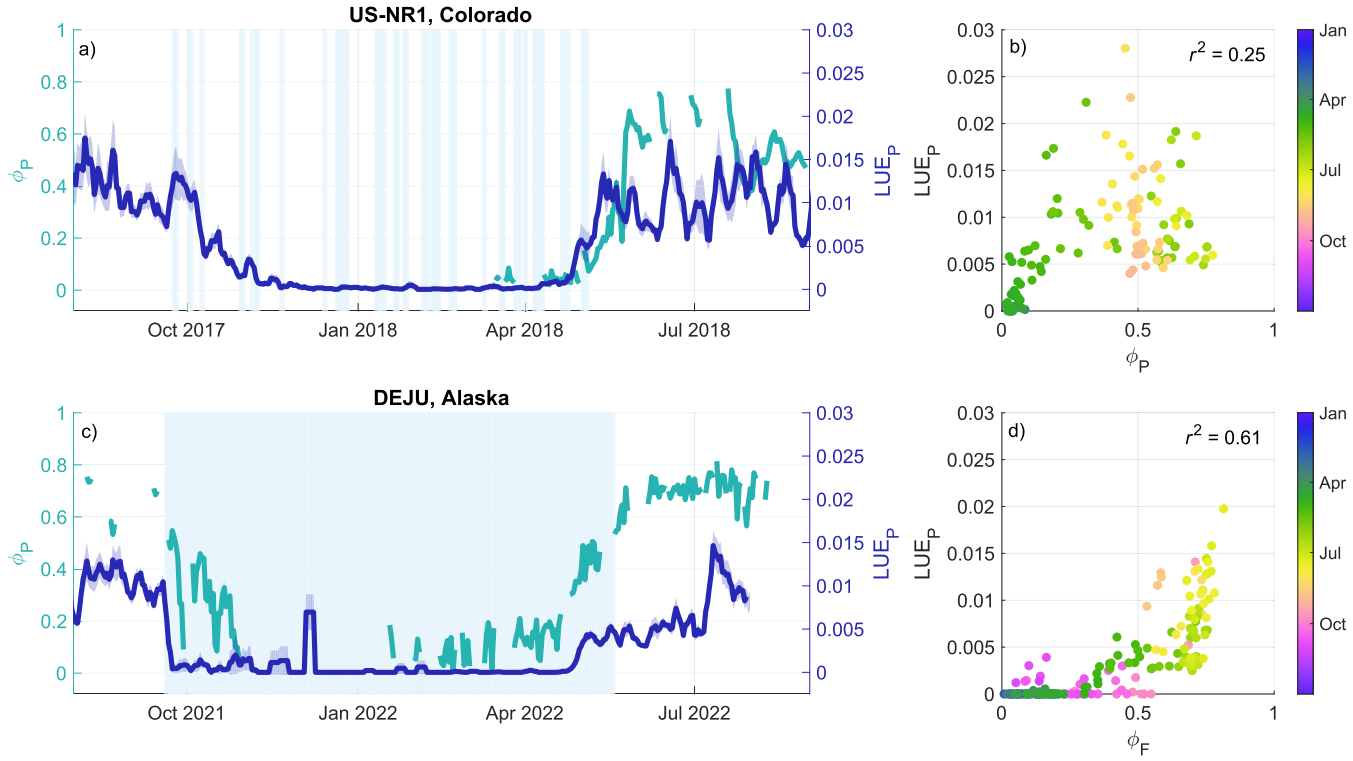


**FIGURE 5** Time series of five-day moving average of tower-based light use efficiency of photosynthesis ($LUE_P$) (dark blue) and daily average needle-scale $\phi_P$ (teal) for US-NR1 (a) and DEJU (c). Scatterplots of daily average $LUE_P$ and $\phi_P$ at US-NR1 (b) and DEJU (d), colored by month of measurement.

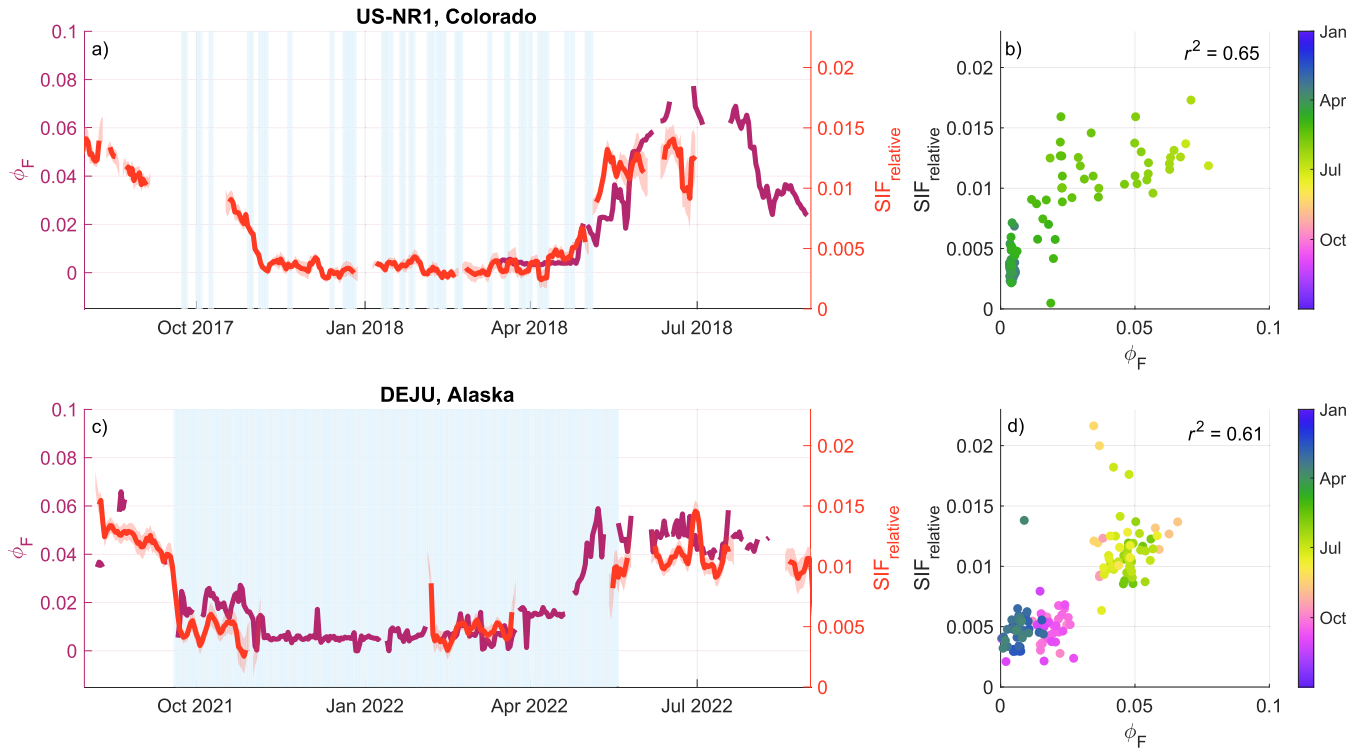


**FIGURE 6** Time series of five-day moving average tower-based $SIF_{relative}$ (light use efficiency of fluorescence [$LUE_F$], red) and daily average needle-scale $\phi_F$ (purple) for US-NR1 (a) and DEJU (c). Scatterplots of daily average $SIF_{relative}$ ($LUE_F$) and $\phi_F$ at US-NR1 (b) and DEJU (d), colored by month of measurement. SIF, solar-induced chlorophyll fluorescence.

transition, but the increase in $SIF_{relative}$ corresponds with the rapid change in $\phi_F$ at US-NR1. The fall transition of $\phi_F$ is captured well with changes in $SIF_{relative}$ at DEJU. Divergence between $SIF_{relative}$ and $\phi_F$ could be driven by several challenges associated with scaling from the leaf to the canopy including differences in the specific trees measured (i.e., footprint differences), radiative transfer within the canopy, and most notably, variability in illumination conditions. Similar to Figure 5, there is more day-to-day variation in the canopy-scale measurements of $SIF_{relative}$ than $\phi_F$ due to more variable light conditions. Nonetheless, both $\phi_F$ and $SIF_{relative}$ are less noisy than $LUE_P$ and $\phi_P$, because steady-state chlorophyll fluorescence typically does not have a strong light response (van der Tol et al., 2016, Figure 7), and is therefore less variable over the course of the day. As a result, we observe a tight correspondence between $SIF_{relative}$ and $\phi_F$ across the season at both sites.

The fluctuations in ENF fluorescence and photochemical yields across seasons are likely connected to shifts in NPQ, brought about by modifications in pigmentation (increased activity of xanthophyll pigments) during the transitions between spring and fall (Ottander et al., 1995). During the fall cessation, adjustments in pigment composition serve to dissipate surplus light energy through sustained NPQ (Adams & Demmig-Adams, 1994). It is well understood that sustained NPQ operates in ecosystems experiencing sub-zero temperatures in winter to suppress both photochemical and fluorescence yields (Müller et al., 2001). The converse happens during the warm season. When light availability increases to potentially saturating levels for photosynthesis and temperatures rise, cold-hardening pigment modifications reverse and lead to a decrease in sustained NPQ. This explanation allows us to scale our understanding of the coordination between photochemical and fluorescence yields to the canopy level (*Remotely sensed fluorescence yield tracks changes in photosynthetic yield*).

## Remotely sensed fluorescence yield tracks changes in photosynthetic yield

Our results show that both $SIF_{relative}$ and $LUE_P$ closely parallel $\phi_F$ and $\phi_P$, respectively over the course of a season, and specifically during the spring onset and fall cessation (Figures 5 and 6). To most effectively use remote sensing metrics to discern photosynthetic phenology we must test the correspondence between tower-based $SIF_{relative}$ and $LUE_P$. To do this, we compare tower-based remote sensing measurements of $SIF_{relative}$ with eddy-covariance derived estimates of $LUE_P$ at each forest (Figures 7 and 8). Across all sites, we observe a rapid increase in $SIF_{relative}$ corresponding with an increase in LUEP during the spring transition (Figure 8). This is particularly evident during the spring of 2018 at US-NR1, spring of 2019 and 2020 at Ca-Obs, and spring 2021 at DEJU. Notably, the increase in $SIF_{relative}$ and $LUE_P$ occur while snow is still present. Additionally, across all sites $SIF_{relative}$ and $LUE_P$ closely follow each other during the fall transition, which is notably a slower transition than what we observe in the spring. Across all three sites, we observe moderately strong relationships between $SIF_{relative}$ and $LUE_P$ at US-NR1 (Figure 8b), Ca-Obs (Figure 8d), and DEJU (Figure 8f).

Despite generally good agreement, there are still several unaccounted sources of divergence between

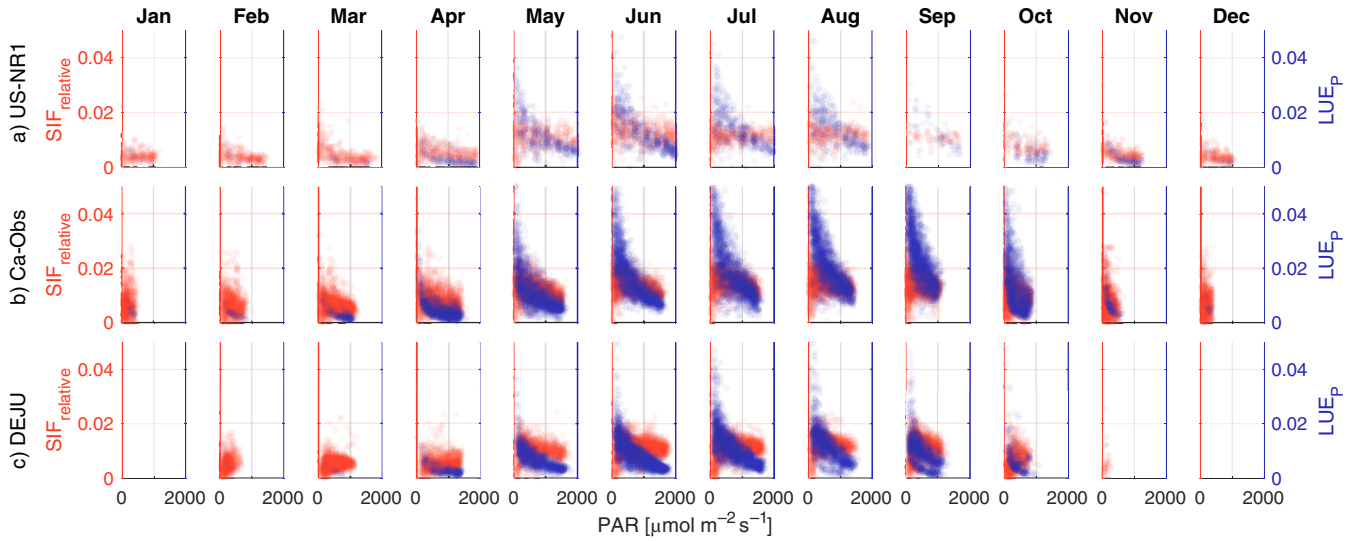


**FIGURE 7** Light response curves of half-hourly $SIF_{relative}$ (red) and light use efficiency of photosynthesis ($LUE_P$) (blue) for each month at US-NR1 (row a), Ca-Obs (row b), and DEJU (row c). SIF, solar-induced chlorophyll fluorescence.

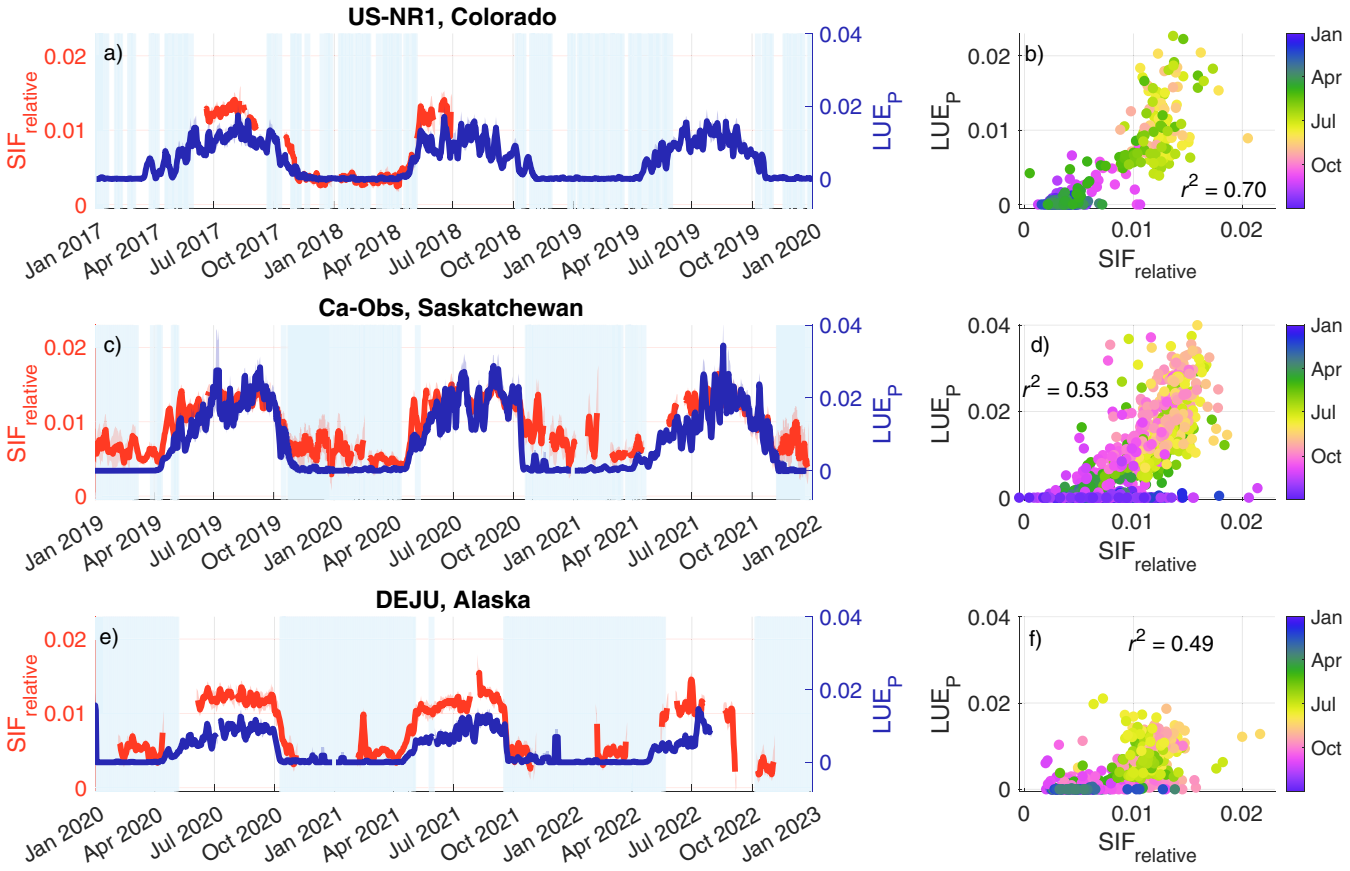


**FIGURE 8** Time series of five-day moving average of tower-based $SIF_{relative}$ (red) and light use efficiency of photosynthesis ($LUE_P$) (blue) over three seasons at US-NR1 (a), Ca-Obs (c), and DEJU (e). Scatterplots of daily average $LUE_P$ and $SIF_{relative}$ at US-NR1 (b), Ca-Obs (d), and DEJU (f), colored by month. SIF, solar-induced chlorophyll fluorescence.

$SIF_{relative}$ and $LUE_P$, that could explain the scatter in our results. Any divergence between $LUE_P$ and $\phi_P$ or $SIF_{relative}$ and $\phi_F$ (as discussed in *Coordination of fluorescence and photosynthetic yields across spatial scales*) will be propagated to divergence in the relationship between $LUE_P$ and $SIF_{relative}$. The different sites also experience differences in illumination conditions that enhance these divergences. For example, at the DEJU site, lower solar zenith angles throughout the growing season, and low PAR values in winter can amplify the challenges in scaling from the leaf to the canopy associated with illumination and radiative transfer within the canopy. This reduces the correlation between $LUE_P$ and $SIF_{relative}$ at the DEJU site when compared with US-NR1or Ca-Obs. Additionally, the sites have different requirements for photoprotection based on the light and temperature environments (Pierrat et al., 2024). US-NR1 experiences sub-zero temperatures in winter while still absorbing appreciable sunlight. In contrast, DEJU experiences similar cold temperatures but is exposed to lower solar irradiance in winter. Therefore, the need for sustained photoprotection over winter will be different across the sites, potentially driving the steepness of the transitions in spring and fall. How each forest transitions into and out of sustained photoprotection will lead to differences between $LUE_P$ and $SIF_{relative}$ that are not yet fully characterized. Even with these potential complications, the success of our approach across sites emphasizes its robustness and highlights where future work could further refine our ability to scale from the leaf to the canopy.

Taken together, these results suggest that $SIF_{relative}$ can account for the impacts of PAR and snow cover on the remotely sensed SIF signal and be used to track photosynthetic phenology in evergreen ecosystems. Using $SIF_{relative}$ to correct for the impact of absorbed light on the SIF signal has previously been demonstrated by Butterfield et al. (2023), who compared tower-based remote sensing data with GPP estimates at a deciduous forest in Michigan. Butterfield et al. (2023) highlight a shared dependence of SIF and GPP on incoming sunlight and show that daily averaged $SIF_{relative}$ better tracks drought conditions than SIF itself. $SIF_{relative}$ will also show minimal response to sunlight diurnally but show a

seasonal cycle, like that of $\phi_F$, $\phi_P$, and LUEP. Light response curves plotted at a monthly timescale (Figure 7) show that $SIF_{relative}$ does not increase with incoming irradiance throughout the day, but shows seasonal changes in its magnitude, with non-zero values in winter. In contrast, $LUE_P$ shows light saturation, seasonal changes coincident with $SIF_{relative}$, and does drop to zero over winter (Figure 7). Given the differing responses of $LUE_P$ and $SIF_{relative}$ to PAR, $SIF_{relative}$ will be ineffective at tracking GPP over the diurnal cycle. Nevertheless, $SIF_{relatvie}$ is an effective proxy for $LUE_F$ and therefore, when averaged to the daily scale can be used to track the seasonal cycle and transitions of $LUE_P$ in ENFs.

Beyond correcting for sunlight, we have demonstrated that SIF and $SIF_{relative}$ are less sensitive to snow (Figure 2), which is particularly relevant as arctic evergreens are known to photosynthesize in early spring even under snow cover (Starr & Oberbauer, 2003), and emergent herbaceous vegetation may initiate photosynthesis prior to snow disappearance (Parazoo et al., 2018). The sensitivity of SIF and $SIF_{relative}$ to snow cover is still a challenge that may be improved with increased modeling efforts; however, $SIF_{relative}$ is an improvement over NIRv. For example, under a 0.5 snow cover fraction we project a ~20% reduction in measured SIF and ~60% reduction in NIRv (Figure 2) making SIF more useful than reflectance-based indices for tracking the start and end of winter dormancy in seasonally snow covered locations. Further, remotely sensed metrics that are robust in the presence of snow cover have greater potential for detecting periodic photosynthetic activity in winter if temperatures are warm enough to thaw stems (Bowling et al., 2018; Pierrat et al., 2021). Precise detection of photosynthetic activity despite the presence of snow is essential for accurate prediction and quantification of the spring transition, that may require changes in parameterization of models which use snowmelt timing as an indicator of carbon uptake in ENFs (Pulliainen et al., 2017). Going forward, applying simple correction techniques that do not rely on ancillary data, or information from the reflectance spectrum, are likely to advance our characterization of physiological activity across space and time in ENFs.

## CONCLUSIONS

In evergreen forests, patterns of temperature and precipitation are changing with climate change, and their collective influence determines the timing of the spring and fall transition seasons—the seasonal arc of photosynthetic activity. It is critical to make field measurements at multiple scales to better interpret remote sensing data for understanding changes in photosynthetic phenology of ENFs. Here, we compared the utility of measurements made at the needle and canopy scale for determining the start and end of photosynthesis in evergreen forests across three ENF sites. Our needle-scale data shows a close co-variation and correlation ($r^2 = 0.74$, 0.70) of fluorescence and photosynthesis across the ENF seasons (Science Question 1). In addition, we observe a seasonal hysteresis where in spring $\phi_F$ and $\phi_P$ increase in parallel and in fall a more rapid decrease in $\phi_F$ is observed, likely driven by changes in sustained NPQ, although more work along these lines is needed. SIF has a lower sensitivity to snow-cover than reflectance-based indices and can thus be used with more confidence when scaling fluorescence and photosynthesis measures from the needle to the canopy in environments with snow (Science Question 2). This is especially important since photosynthetic activity begins prior to spring snowmelt across our three study sites (Bowling et al., 2024; Desai et al., 2011). Over winter, SIF maintains a limited light response and does not decline to zero while GPP does, therefore, illumination effects must be considered when using SIF as a phenological metric. We can do this using $SIF_{relative}$, which shows strong performance for overcoming challenges associated with disentangling the physiological from the physical effects on SIF (illumination and snow) because it does not rely on ancillary data, or information from the reflectance spectrum. We show that our needle-scale observations correspond to the site-level with tower-based estimates of $LUE_P$ and $SIF_{relative}$ which also show a good correlation across all sites ($r^2 = 0.70$, 0.53, 0.49). Our results demonstrate the mechanistic underpinnings of what SIF data can (and cannot) tell us about seasonal transitions in ENF photosynthesis and important considerations and corrections that can be applied to improve the utility of these data. Although this study focused on ENFs, our findings are highly relevant for other ecosystems. Seasonal snow cover complicating remote sensing observations is not unique to ENFs, and we have highlighted the advantages of SIF in addressing this issue. While we show good agreement between fluorescence and photosynthetic yields across scales and ENF sites, our multi-scale experimental setup is one that can be applied in other ecosystems. Because observations of SIF can be made from spaceborne platforms, our approach has considerable potential to improve monitoring of biological processes in ecosystems globally. Given its sensitivity to photosynthetic phenology, the nearly 30 years of a multi-sensor satellite SIF record (Sun et al., 2023), efforts to harmonize spaceborne records (Parazoo et al., 2019) and integrate within land surface models (Parazoo et al., 2020), our results support SIF as a climate variable which should be continued to be measured routinely across space agencies and scales.

## ACKNOWLEDGMENTS

We would like to thank the reviewers and editors whose feedback helped improve this manuscript. We would also like to thank the field technicians and site PIs for their support. Russell Doughty was supported by NASA Making Earth System data Records for Use in Research Environments (MEaSUREs) Program (NNN12AA01C). Zoe Amie Pierrat and Andrew Maguire were supported by an appointment to the NASA Postdoctoral Program at the Jet Propulsion Laboratory. This material is also based upon work supported by the National Science Foundation Graduate Research Fellowship under Grant Nos. DGE-1650604 and DGE2034835. Any opinion, findings, and conclusions or recommendations expressed in this material are those of the authors(s) and do not necessarily reflect the views of the National Science Foundation. We would, additionally, like to acknowledge support from the National Science Foundation Macrosystems Biology and NEON-Enabled Science (Award 1926090), and National Science Foundation (Award 1929709). We would also like to acknowledge NASA ABoVE programs award #80NSSC19M0133. A portion of this research was carried out at the Jet Propulsion Laboratory, California Institute of Technology, under a contract with the National Aeronautics and Space Administration. 

## CONFLICT OF INTEREST STATEMENT

The authors declare no conflicts of interest.

## DATA AVAILABILITY STATEMENT

Needle and canopy-scale fluorescence data at US-NR1 (Magney, Bowling, et al., 2019; Magney, Frankenberg, et al., 2019) are available from CaltechDATA at https://doi.org/10.22002/D1.1231. All other data (Pierrat, 2023) are available in Zenodo at https://doi.org/10.5281/zenodo.10048769.

## ORCID

*Zoe Amie Pierrat* https://orcid.org/0000-0002-6726-2406
*Troy Magney* https://orcid.org/0000-0002-9033-0024
*Andrew Maguire* https://orcid.org/0000-0002-6334-0497
*Logan Brissette* https://orcid.org/0000-0001-8290-5900
*Russell Doughty* https://orcid.org/0000-0001-5191-2155
*David R. Bowling* https://orcid.org/0000-0002-3864-4042
*Barry Logan* https://orcid.org/0000-0003-3920-2139
*Nicholas Parazoo* https://orcid.org/0000-0002-4165-4532
*Christian Frankenberg* https://orcid.org/0000-0002-0546-5857
*Jochen Stutz* https://orcid.org/0000-0001-6368-7629

## REFERENCES

Adams, W. W., and B. Demmig-Adams. 1994. "Carotenoid Composition and Down Regulation of Photosystem II in Three Conifer Species during the Winter." *Physiologia Plantarum* 92: 451–58. https://doi.org/10.1111/j.1399-3054.1994.tb08835.x.

Adams, W. W., C. R. Zarter, V. Ebbert, and B. Demmig-Adams. 2004. "Photoprotective Strategies of Overwintering Evergreens." *BioScience* 54: 41–49. https://doi.org/10.1641/0006-3568(2004)054[0041:psooe]2.0.co;2.

Badgley, G., L. D. L. Anderegg, J. A. Berry, and C. B. Field. 2019. "Terrestrial Gross Primary Production: Using NIRV to Scale from Site to Globe." *Global Change Biology* 25: 3731–40. https://doi.org/10.1111/gcb.14729.

Badgley, G., C. B. Field, and J. A. Berry. 2017. "Canopy Near-Infrared Reflectance and Terrestrial Photosynthesis." *Science Advances* 3: e1602244. https://doi.org/10.1126/sciadv.1602244.

Baldocchi, D. D. 2003. "Assessing the Eddy Covariance Technique for Evaluating Carbon Dioxide Exchange Rates of Ecosystems: Past, Present and Future." *Global Change Biology* 9: 479–492. https://doi.org/10.1046/j.1365-2486.2003.00629.x.

Baldridge, A. M., S. J. Hook, C. I. Grove, and G. Rivera. 2009. "The ASTER Spectral Library Version 2.0." *Remote Sensing of Environment* 113: 711–15. https://doi.org/10.1016/j.rse.2008.11.007.

Barber, J., S. Malkin, A. Telfer, U. Schreiber, D. A. Walker, and C. B. Osmond. 1997. "The Origin of Chlorophyll Fluorescence in Vivo and Its Quenching by the Photosystem II Reaction Centre." *Philosophical Transactions of the Royal Society of London. B, Biological Sciences* 323: 227–239. https://doi.org/10.1098/rstb.1989.0006.

Barr, A. G., T. A. Black, E. H. Hogg, N. Kljun, K. Morgenstern, and Z. Nesic. 2004. "Inter-Annual Variability in the Leaf Area Index of a Boreal Aspen-Hazelnut Forest in Relation to Net Ecosystem Production." *Agricultural and Forest Meteorology* 126: 237–255. https://doi.org/10.1016/j.agrformet.2004.06.011.

Barr, A. G., K. Morgenstern, T. A. Black, J. H. McCaughey, and Z. Nesic. 2006. "Surface Energy Balance Closure by the Eddy-Covariance Method above Three Boreal Forest Stands and Implications for the Measurement of the $CO_2$ Flux." *Agricultural and Forest Meteorology* 140: 322–337. https://doi.org/10.1016/j.agrformet.2006.08.007.

Barton, C. V. M., and P. R. J. North. 2001. "Remote Sensing of Canopy Light Use Efficiency Using the Photochemical Reflectance Index: Model and Sensitivity Analysis." *Remote Sensing of Environment* 78: 264–273. https://doi.org/10.1016/S0034-4257(01)00224-3.

Bonan, G. B. 2008. "Forests and Climate Change: Forcings, Feedbacks, and the Climate Benefits of Forests." *Science* 320: 1444–49. https://doi.org/10.1126/science.1155121.

Bowling, D. R., B. A. Logan, K. Hufkens, D. M. Aubrecht, A. D. Richardson, S. P. Burns, W. R. L. Anderegg, P. D. Blanken, and D. P. Eiriksson. 2018. "Limitations to Winter and Spring Photosynthesis of a Rocky Mountain Subalpine Forest." *Agricultural and Forest Meteorology* 252: 241–255. https://doi.org/10.1016/j.agrformet.2018.01.025.

Bowling, D. R., C. Schädel, K. R. Smith, A. D. Richardson, M. Bahn, M. A. Arain, A. Varlagin, et al. 2024. "Phenology of Photosynthesis in Winter-Dormant Temperate and Boreal Forests: Long-Term Observations from Flux Towers and

Quantitative Evaluation of Phenology Models." *Journal of Geophysical Research: Biogeosciences* 129: e2023JG007839. https://doi.org/10.1029/2023JG007839.

Burns, S. P., P. D. Blanken, A. A. Turnipseed, J. Hu, and R. K. Monson. 2015. "The Influence of Warm-Season Precipitation on the Diel Cycle of the Surface Energy Balance and Carbon Dioxide at a Colorado Subalpine Forest Site." *Biogeosciences* 12: 7349–77. https://doi.org/10.5194/bg-12-7349-2015.

Butterfield, Z., T. Magney, K. Grossmann, G. Bohrer, C. Vogel, S. Barr, and G. Keppel-Aleks. 2023. "Accounting for Changes in Radiation Improves the Ability of SIF to Track Water Stress-Induced Losses in Summer GPP in a Temperate Deciduous Forest. Journal of Geophysical Research." *Biogeosciences* 128: e2022JG007352. https://doi.org/10.1029/2022JG007352.

Chang, C. Y., L. Guanter, C. Frankenberg, P. Köhler, L. Gu, T. S. Magney, K. Grossmann, and Y. Sun. 2020. "Systematic Assessment of Retrieval Methods for Canopy Far-Red Solar-Induced Chlorophyll Fluorescence Using High-Frequency Automated Field Spectroscopy." *Journal of Geophysical Research: Biogeosciences* 125: e2019JG005533. https://doi.org/10.1029/2019JG005533/FORMAT/PDF.

Chen, J. M., A. Govind, O. Sonnentag, Y. Zhang, A. Barr, and B. Amiro. 2006. "Leaf Area Index Measurements at Fluxnet-Canada Forest Sites." *Agricultural and Forest Meteorology* 140: 257–268. https://doi.org/10.1016/j.agrformet.2006.08.005.

Cheng, R., T. S. Magney, D. Dutta, D. R. Bowling, B. A. Logan, S. P. Burns, P. D. Blanken, et al. 2020. "Decomposing Reflectance Spectra to Track Gross Primary Production in a Subalpine Evergreen Forest." *Biogeosciences* 17: 4523–44. https://doi.org/10.5194/bg-17-4523-2020.

Cheng, R., T. S. Magney, E. L. Orcutt, Z. Pierrat, P. Köhler, D. R. Bowling, M. S. Bret-Harte, et al. 2022. "Evaluating Photosynthetic Activity across Arctic-Boreal Land Cover Types Using Solar-Induced Fluorescence." *Environmental Research Letters* 17: 115009.

Dechant, B., Y. Ryu, G. Badgley, Y. Zeng, J. A. Berry, Y. Zhang, Y. Goulas, et al. 2020. "Canopy Structure Explains the Relationship between Photosynthesis and Sun-Induced Chlorophyll Fluorescence in Crops." *Remote Sensing of Environment* 241: 111733. https://doi.org/10.1016/j.rse.2020.111733.

Delta Junction NEON|NSF NEON. n.d. "Open Data to Understand Our Ecosystems [WWW Document]." https://www.neonscience.org/field-sites/deju.

Desai, A. R., D. J. P. Moore, W. K. M. Ahue, P. T. V. Wilkes, S. F. J. De Wekker, B. G. Brooks, T. L. Campos, et al. 2011. "Seasonal Pattern of Regional Carbon Balance in the Central Rocky Mountains from Surface and Airborne Measurements." *Journal of Geophysical Research: Biogeosciences* 116. https://doi.org/10.1029/2011JG001655.

Dye, D. G., and C. J. Tucker. 2003. "Seasonality and Trends of Snow-Cover, Vegetation Index, and Temperature in Northern Eurasia." *Geophysical Research Letters* 30. https://doi.org/10.1029/2002GL016384.

Ensminger, I., D. Sveshnikov, D. A. Campbell, C. Funk, S. Jansson, J. Lloyd, O. Shibistova, and G. Öquist. 2004. "Intermittent Low Temperatures Constrain Spring Recovery of Photosynthesis in Boreal Scots Pine Forests." *Global Change Biology* 10: 995–1008. https://doi.org/10.1111/j.1365-2486.2004.00781.x.

Ensminger, I., M. Xyländer, C. Hagen, and W. Braune. 2001. "Strategies Providing Success in a Variable Habitat: III. Dynamic Control of Photosynthesis in *Cladophora glomerata*." *Plant, Cell & Environment* 24: 769–779. https://doi.org/10.1046/j.1365-3040.2001.00725.x.

Fisher, J. B., D. J. Hayes, C. R. Schwalm, D. N. Huntzinger, E. Stofferahn, K. Schaefer, Y. Luo, et al. 2018. "Missing Pieces to Modeling the Arctic-Boreal Puzzle." *Environmental Research Letters* 13: 020202. https://doi.org/10.1088/1748-9326/aa9d9a.

Frankenberg, C., and J. Berry. 2017. "Solar Induced Chlorophyll Fluorescence: Origins, Relation to Photosynthesis and Retrieval." *Comprehensive Remote Sensing* 1–9: 143–162. https://doi.org/10.1016/B978-0-12-409548-9.10632-3.

Fu, Z., P. C. Stoy, Y. Luo, J. Chen, J. Sun, L. Montagnani, G. Wohlfahrt, et al. 2017. "Climate Controls over the Net Carbon Uptake Period and Amplitude of Net Ecosystem Production in Temperate and Boreal Ecosystems." *Agricultural and Forest Meteorology* 243: 9–18. https://doi.org/10.1016/j.agrformet.2017.05.009.

Galbavy, E. S., C. Anastasio, B. L. Lefer, and S. R. Hall. 2007. "Light Penetration in the Snowpack at Summit, Greenland: Part 1: Nitrite and Hydrogen Peroxide Photolysis." *Atmospheric Environment* 41: 5077–90. https://doi.org/10.1016/j.atmosenv.2006.04.072.

Goetz, S. J., A. G. Bunn, G. J. Fiske, and R. A. Houghton. 2005. "Satellite-Observed Photosynthetic Trends across Boreal North America Associated with Climate and Fire Disturbance." *Proceedings of the National Academy of Sciences of the United States of America* 102: 13521–25. https://doi.org/10.1073/pnas.0506179102.

Grossmann, K., C. Frankenberg, T. S. Magney, S. C. Hurlock, U. Seibt, and J. Stutz. 2018. "PhotoSpec: A New Instrument to Measure Spatially Distributed Red and Far-Red Solar-Induced Chlorophyll Fluorescence." *Remote Sensing of Environment* 216: 311–327. https://doi.org/10.1016/j.rse.2018.07.002.

Guanter, L., Y. Zhang, M. Jung, J. Joiner, M. Voigt, J. A. Berry, C. Frankenberg, et al. 2014. "Global and Time-Resolved Monitoring of Crop Photosynthesis with Chlorophyll Fluorescence." *Proceedings of the National Academy of Sciences of the United States of America* 111: E1327–E1333. https://doi.org/10.1073/PNAS.1320008111.

Guidi, L., M. Tattini, M. Landi, L. Guidi, M. Tattini, and M. Landi. 2017. "How Does Chloroplast Protect Chlorophyll against Excessive Light?" In *Chlorophyll*, edited by E. Jacob-Lopes, L. Queiroz Zepka, and M. I. Queiroz, 21–36. London: IntechOpen. https://doi.org/10.5772/67887.

Heinz Walz GmbH. 2023. "MONI-HEAD MONI-DA Manual." https://www.htsperu.com.pe/download/Manual-Moni-Da-ICT-INTERNATIONAL.mJ7KUimhliqRBXSoCgUpkiJLJ9PolQCb.pdf.

Hollinger, D. Y., and A. D. Richardson. 2005. "Uncertainty in Eddy Covariance Measurements and Its Application to Physiological Models." *Tree Physiology* 25: 873–885. https://doi.org/10.1093/treephys/25.7.873.

Hu, J., D. J. P. Moore, S. P. Burns, and R. K. Monson. 2010. "Longer Growing Seasons Lead to Less Carbon Sequestration by a Subalpine Forest." *Global Change Biology* 16: 771–783. https://doi.org/10.1111/j.1365-2486.2009.01967.x.

Jarvis, P. G., J. M. Massheder, S. E. Hale, J. B. Moncrieff, M. Rayment, and S. L. Scott. 1997. "Seasonal Variation of Carbon Dioxide, Water Vapor, and Energy Exchanges of a Boreal Black Spruce Forest." *Journal of Geophysical Research Atmospheres* 102: 28953–66. https://doi.org/10.1029/97jd01176.

Jeong, S. J., C. H. Ho, H. J. Gim, and M. E. Brown. 2011. "Phenology Shifts at Start Vs. End of Growing Season in Temperate Vegetation over the Northern Hemisphere for the Period 1982-2008." *Global Change Biology* 17: 2385–99. https://doi.org/10.1111/j.1365-2486.2011.02397.x.

Jeong, S. J., D. Schimel, C. Frankenberg, D. T. Drewry, J. B. Fisher, M. Verma, J. A. Berry, J. E. Lee, and J. Joiner. 2017. "Application of Satellite Solar-Induced Chlorophyll Fluorescence to Understanding Large-Scale Variations in Vegetation Phenology and Function over Northern High Latitude Forests." *Remote Sensing of Environment* 190: 178–187. https://doi.org/10.1016/j.rse.2016.11.021.

Kim, J., Y. Ryu, B. Dechant, H. Lee, H. Seok, A. Kornfeld, and J. A. Berry. 2021. "Remote Sensing of Environment Solar-Induced Chlorophyll Fluorescence Is Non-Linearly Related to Canopy Photosynthesis in a Temperate Evergreen Needleleaf Forest during the Fall Transition." *Remote Sensing of Environment* 258: 112362. https://doi.org/10.1016/j.rse.2021.112362.

Kimm, H., K. Guan, C. Jiang, G. Miao, G. Wu, A. E. Suyker, E. A. Ainsworth, et al. 2021. "A Physiological Signal Derived from Sun-Induced Chlorophyll Fluorescence Quantifies Crop Physiological Response to Environmental Stresses in the U.S. Corn Belt." *Environmental Research Letters* 16: 124051. https://doi.org/10.1088/1748-9326/ac3b16.

Kolari, P., H. K. Lappalainen, H. Hänninen, and P. Hari. 2007. "Relationship between Temperature and the Seasonal Course of Photosynthesis in Scots Pine at Northern Timberline and in Southern Boreal Zone." *Tellus B: Chemical and Physical Meteorology* 59: 542–552. https://doi.org/10.1111/j.1600-0889.2007.00262.x.

Lasslop, G., M. Reichstein, D. Papale, A. Richardson, A. Arneth, A. Barr, P. Stoy, and G. Wohlfahrt. 2010. "Separation of Net Ecosystem Exchange into Assimilation and Respiration Using a Light Response Curve Approach: Critical Issues and Global Evaluation." *Global Change Biology* 16: 187–208. https://doi.org/10.1111/j.1365-2486.2009.02041.x.

Lundmark, T., J. Bergh, M. Strand, and A. Koppel. 1998. "Seasonal Variation of Maximum Photochemical Efficiencyin Boreal NorwaySpruce Stands." *Trees* 13: 63–67. https://doi.org/10.1007/s004680050187.

Magney, T., C. Frankenberg, K. Grossmann, D. Bowling, B. Logan, S. Burns, and J. Stutz. 2019. "Canopy and Needle Scale Fluorescence Data from Niwot Ridge, Colorado 2017-2018 (1.2) [Data set]." CaltechDATA. https://doi.org/10.22002/D1.1231.

Magney, T. S., M. L. Barnes, and X. Yang. 2020. "On the Covariation of Chlorophyll Fluorescence and Photosynthesis across Scales." *Geophysical Research Letters* 47: e2020GL091098. https://doi.org/10.1029/2020gl091098.

Magney, T. S., D. R. Bowling, B. A. Logan, K. Grossmann, J. Stutz, P. D. Blanken, S. P. Burns, et al. 2019. "Mechanistic Evidence for Tracking the Seasonality of Photosynthesis with Solar-Induced Fluorescence." *Proceedings of the National Academy of Sciences of the United States of America* 116: 11640–45. https://doi.org/10.1073/pnas.1900278116.

Maguire, A. J., J. U. H. Eitel, K. L. Griffin, T. S. Magney, R. A. Long, L. A. Vierling, S. C. Schmiege, et al. 2020. "On the Functional Relationship between Fluorescence and Photochemical Yields in Complex Evergreen Needleleaf Canopies." *Geophysical Research Letters* 47: e2020GL087858. https://doi.org/10.1029/2020GL087858.

Maguire, A. J., J. U. H. Eitel, T. S. Magney, C. Frankenberg, P. Köhler, E. L. Orcutt, N. C. Parazoo, R. Pavlick, and Z. A. Pierrat. 2021. "Spatial Covariation between Solar-Induced Fluorescence and Vegetation Indices from Arctic-Boreal Landscapes." *Environmental Research Letters* 16: 095002. https://doi.org/10.1088/1748-9326/ac188a.

Martini, D., K. Sakowska, G. Wohlfahrt, J. Pacheco-Labrador, C. van der Tol, A. Porcar-Castell, T. S. Magney, et al. 2022. "Heatwave Breaks down the Linearity between Sun-Induced Fluorescence and Gross Primary Production." *New Phytologist* 233: 2415–28. https://doi.org/10.1111/nph.17920.

Maxwell, K., and G. N. Johnson. 2000. "Chlorophyll Fluorescence – A Practical Guide." *Journal of Experimental Botany* 51: 659–668. https://doi.org/10.1093/jxb/51.345.659.

Mohammed, G. H., R. Colombo, E. M. Middleton, U. Rascher, C. van der Tol, L. Nedbal, Y. Goulas, et al. 2019. "Remote Sensing of Solar-Induced Chlorophyll Fluorescence (SIF) in Vegetation: 50 Years of Progress." *Remote Sensing of Environment* 231: 111177. https://doi.org/10.1016/j.rse.2019.04.030.

Monson, R. K., M. R. Prater, J. Hu, S. P. Burns, J. P. Sparks, K. L. Sparks, and L. E. Scott-Denton. 2010. "Tree Species Effects on Ecosystem Water-Use Efficiency in a High-Elevation, Subalpine Forest." *Oecologia* 162: 491–504. https://doi.org/10.1007/s00442-009-1465-z.

Müller, P., X. P. Li, and K. K. Niyogi. 2001. "Non-Photochemical Quenching. A Response to Excess Light Energy." *Plant Physiology* 125: 1558–66. https://doi.org/10.1104/pp.125.4.1558.

Murchie, E. H., and T. Lawson. 2013. "Chlorophyll Fluorescence Analysis: AGuide to Good Practice and Understanding Some New Applications." *Journal of Experimental Botany* 64: 3983–98. https://doi.org/10.1093/jxb/ert208.

National Ecological Observatory Network (NEON). 2022. "Bundled Data Products – Eddy Covariance (DP4.00200.001): RELEASE-2022." https://doi.org/10.48443/7CQP-3J73.

Nehemy, M. F., Z. Pierrat, J. Maillet, A. D. Richardson, J. Stutz, B. Johnson, W. Helgason, A. G. Barr, C. P. Laroque, and J. J. McDonnell. 2023. "Phenological Assessment of Transpiration: The Stem-Temp Approach for Determining Start and End of Season." *Agricultural and Forest Meteorology* 331: 109319. https://doi.org/10.1016/j.agrformet.2023.109319.

Nelson, P. R., A. J. Maguire, Z. Pierrat, E. L. Orcutt, D. Yang, S. Serbin, G. V. Frost, et al. 2022. "Remote Sensing of Tundra Ecosystems Using High Spectral Resolution Reflectance: Opportunities and Challenges." *Journal of Geophysical Research: Biogeosciences* 127: e2021JG006697. https://doi.org/10.1029/2021JG006697.

Nichol, C. J., K. F. Huemmrich, T. A. Black, P. G. Jarvis, C. L. Walthall, J. Grace, and F. G. Hall. 2000. "Remote Sensing of Photosynthetic-Light-Use Efficiency of Boreal Forest." *Agricultural and Forest Meteorology* 101: 131–142. https://doi.org/10.1016/S0168-1923(99)00167-7.

Öquist, G. 1983. "Effects of Low Temperature on Photosynthesis." *Plant, Cell & Environment* 6: 281–300. https://doi.org/10.1111/1365-3040.ep11612087.

Öquist, G., and N. P. A. Huner. 2003. "Photosynthesis of Overwintering Evergreen Plants." *Annual Review of Plant Biology* 54: 329–355. https://doi.org/10.1146/annurev.arplant.54.072402.115741.

Ottander, C., D. Campbell, and G. Öquist. 1995. "Seasonal Changes in Photosystem II Organisation and Pigment Composition in *Pinus sylvestris*." *Planta* 197: 176–183. https://doi.org/10.1007/BF00239954.

Parazoo, N. C., A. Arneth, T. A. M. Pugh, B. Smith, N. Steiner, K. Luus, R. Commane, et al. 2018. "Spring Photosynthetic Onset and Net $CO_2$ Uptake in Alaska Triggered by Landscape Thawing." *Global Change Biology* 24: 3416–35. https://doi.org/10.1111/gcb.14283.

Parazoo, N. C., C. Frankenberg, P. Köhler, J. Joiner, Y. Yoshida, T. Magney, Y. Sun, and V. Yadav. 2019. "Towards a Harmonized Long-Term Spaceborne Record of Far-Red Solar-Induced Fluorescence." *Journal of Geophysical Research: Biogeosciences* 124: 2518–39. https://doi.org/10.1029/2019JG005289.

Parazoo, N. C., T. S. Magney, A. Norton, B. Raczka, C. Bacour, F. Maignan, I. Baker, et al. 2020. "Wide Discrepancies in the Magnitude and Direction of Modelled SIF in Response to Light Conditions." *Biogeosciences* 17: 3733–3733. https://doi.org/10.5194/bg-2019-508.

Pierrat, Z. 2023. "Evergreen Needleleaf Forest Pigment, MONI-PAM, Eddy-Covariance, and Tower-Scale Remote Sensing Data across Four Different Sites [Data Set]." BioScience. Zenodo. https://doi.org/10.5281/zenodo.10048770.

Pierrat, Z., T. Magney, N. C. Parazoo, K. Grossmann, D. R. Bowling, U. Seibt, B. Johnson, et al. 2022. "Diurnal and Seasonal Dynamics of Solar-Induced Chlorophyll Fluorescence, Vegetation Indices, and Gross Primary Productivity in the Boreal Forest. Journal of Geophysical Research." *Biogeosciences* 127: e2021JG006588. https://doi.org/10.1029/2021JG006588.

Pierrat, Z., M. F. Nehemy, A. Roy, T. Magney, N. C. Parazoo, C. Laroque, C. Pappas, et al. 2021. "Tower-Based Remote Sensing Reveals Mechanisms behind a Two-Phased Spring Transition in a Mixed-Species Boreal Forest." *Journal of Geophysical Research: Biogeosciences* 126: 1–20. https://doi.org/10.1029/2020JG006191.

Pierrat, Z. A., J. Bortnik, B. Johnson, A. Barr, T. Magney, D. R. Bowling, N. Parazoo, C. Frankenberg, U. Seibt, and J. Stutz. 2022. "Forests for Forests: Combining Vegetation Indices with Solar-Induced Chlorophyll Fluorescence in Random Forest Models Improves Gross Primary Productivity Prediction in the Boreal Forest." *Environmental Research Letters* 17: 125006. https://doi.org/10.1088/1748-9326/aca5a0.

Pierrat, Z. A., T. S. Magney, R. Cheng, A. J. Maguire, C. Y. S. Wong, M. F. Nehemy, M. Rao, et al. 2024. "The Biological Basis for Using Optical Signals to Track Evergreen Needleleaf Photosynthesis." *BioScience* 73: biad116. https://doi.org/10.1093/biosci/biad116.

Porcar-Castell, A. 2011. "A High-Resolution Portrait of the Annual Dynamics of Photochemical and Non-Photochemical Quenching in Needles of *Pinus sylvestris*." *Physiologia Plantarum* 143: 139–153. https://doi.org/10.1111/j.1399-3054.2011.01488.x.

Porcar-Castell, A., E. Juurola, E. Nikinmaa, F. Berninger, I. Ensminger, and P. Hari. 2008. "Seasonal Acclimation of Photosystem II in *Pinus sylvestris*. I. Estimating the Rate Constants of Sustained Thermal Energy Dissipation and Photochemistry." *Tree Physiology* 28: 1475–82. https://doi.org/10.1093/treephys/28.10.1475.

Porcar-Castell, A., Z. Malenovský, T. Magney, S. Van Wittenberghe, B. Fernández-Marín, F. Maignan, Y. Zhang, et al. 2021. "Chlorophyll a Fluorescence Illuminates a Path Connecting Plant Molecular Biology to Earth-System Science." *Nature Plants* 7: 998–1009. https://doi.org/10.1038/s41477-021-00980-4.

Porcar-Castell, A., E. Tyystjärvi, J. Atherton, C. Van Der Tol, J. Flexas, E. E. Pfündel, J. Moreno, C. Frankenberg, and J. A. Berry. 2014. "Linking Chlorophyll a Fluorescence to Photosynthesis for Remote Sensing Applications: Mechanisms and Challenges." *Journal of Experimental Botany* 65: 4065–95. https://doi.org/10.1093/jxb/eru191.

Pulliainen, J., M. Aurela, T. Laurila, T. Aalto, M. Takala, M. Salminen, M. Kulmala, et al. 2017. "Early Snowmelt Significantly Enhances Boreal Springtime Carbon Uptake." *Proceedings of the National Academy of Sciences of the United States of America* 114: 11081–86. https://doi.org/10.1073/pnas.1707889114.

Richardson, A. D., T. A. Black, P. Ciais, N. Delbart, M. A. Friedl, N. Gobron, D. Y. Hollinger, et al. 2010. "Influence of Spring and Autumn Phenological Transitions on Forest Ecosystem Productivity." *Philosophical Transactions of the Royal Society B: Biological Sciences* 365: 3227–46. https://doi.org/10.1098/rstb.2010.0102.

Schaefer, K., H. Lantuit, V. E. Romanovsky, E. A. G. Schuur, and R. Witt. 2014. "The Impact of the Permafrost Carbon Feedback on Global Climate." *Environmental Research Letters* 9: 085003. https://doi.org/10.1088/1748-9326/9/8/085003.

Sevanto, S., T. Suni, J. Pumpanen, T. Grönholm, P. Kolari, E. Nikinmaa, P. Hari, and T. Vesala. 2006. "Wintertime Photosynthesis and Water Uptake in a Boreal Forest." *Tree Physiology* 26: 749–757. https://doi.org/10.1093/treephys/26.6.749.

Sims, D. A., A. F. Rahman, V. D. Cordova, B. Z. El-Masri, D. D. Baldocchi, L. B. Flanagan, A. H. Goldstein, et al. 2006. "On the Use of MODIS EVI to Assess Gross Primary Productivity of North American Ecosystems." *Journal of Geophysical Research: Biogeosciences* 111. https://doi.org/10.1029/2006JG000162.

Springer, K. R., R. Wang, and J. A. Gamon. 2017. "Parallel Seasonal Patterns of Photosynthesis, Fluorescence, and Reflectance Indices in Boreal Trees." *Remote Sensing* 9: 691. https://doi.org/10.3390/rs9070691.

Starr, G., and S. F. Oberbauer. 2003. "Photosynthesisof Arctic Evergreensunder Snow: Implications for Tundra Ecosystem Carbon Balance." *Ecology* 84: 1415–20. https://doi.org/10.1890/02-3154.

Sun, Y., C. Frankenberg, J. D. Wood, D. S. Schimel, M. Jung, L. Guanter, D. T. Drewry, et al. 2017. "OCO-2 Advances Photosynthesis Observation from Space Via Solar-Induced Chlorophyll Fluorescence." *Science* 358: eaam5747. https://doi.org/10.1126/science.aam5747.

Sun, Y., J. Wen, L. Gu, J. Joiner, C. Y. Chang, C. van der Tol, A. Porcar-Castell, et al. 2023. "From Remotely-Sensed Solar-Induced Chlorophyll Fluorescence to Ecosystem Structure, Function, and Service: Part II—Harnessing Data." *Global Change Biology* 29: 2893–2925. https://doi.org/10.1111/gcb.16646.

Suyker, A. E., S. B. Verma, G. G. Burba, T. J. Arkebauer, D. T. Walters, and K. G. Hubbard. 2004. "Growing Season Carbon Dioxide Exchange in Irrigated and Rainfed Maize." *Agricultural and Forest Meteorology* 124: 1–13. https://doi.org/10.1016/j.agrformet.2004.01.011.

Thurner, M., C. Beer, M. Santoro, N. Carvalhais, T. Wutzler, D. Schepaschenko, A. Shvidenko, et al. 2014. "Carbon Stock and Density of Northern Boreal and Temperate Forests." *Global Ecology and Biogeography* 23: 297–310. https://doi.org/10.1111/geb.12125.

van der Tol, C., M. Rossini, S. Cogliati, W. Verhoef, R. Colombo, U. Rascher, and G. Mohammed. 2016. "A Model and Measurement Comparison of Diurnal Cycles of Sun-Induced Chlorophyll Fluorescence of Crops." *Remote Sensing of Environment* 186: 663–677. https://doi.org/10.1016/j.rse.2016.09.021.

Verhoeven, A. 2014. "Sustained Energy Dissipation in Winter Evergreens." *New Phytologist* 201: 57–65. https://doi.org/10.1111/nph.12466.

Walter-McNeill, A., M. A. Garcia, B. A. Logan, D. M. Bombard, J. S. Reblin, S. Lopez, C. D. Southwick, E. L. Sparrow, and D. R. Bowling. 2021. "Wide Variation of Winter-Induced Sustained Thermal Energy Dissipation in Conifers: ACommon-Garden Study." *Oecologia* 197(3): 589–598. https://doi.org/10.1007/S00442-021-05038-Y.

Wang, R., K. R. Springer, and J. A. Gamon. 2023. "Confounding Effects of Snow Cover on Remotely Sensed Vegetation Indices of Evergreen and Deciduous Trees: An Experimental Study." *Global Change Biology* 29: 6120–38. https://doi.org/10.1111/gcb.16916.

Wutzler, T., A. Lucas-Moffat, M. Migliavacca, J. Knauer, K. Sickel, L. Šigut, O. Menzer, and M. Reichstein. 2018. "Basic and Extensible Post-Processing of Eddy Covariance Flux Data with REddyProc." *Biogeosciences* 15: 5015–30. https://doi.org/10.5194/bg-15-5015-2018.

Yang, J. C., T. S. Magney, L. P. Albert, A. D. Richardson, C. Frankenberg, J. Stutz, K. Grossmann, et al. 2022. "Gross Primary Production (GPP) and Red Solar Induced Fluorescence (SIF) Respond Differently to Light and Seasonal Environmental Conditions in a Subalpine Conifer Forest." *Agricultural and Forest Meteorology* 317: 108904. https://doi.org/10.1016/J.AGRFORMET.2022.108904.

Yang, P., C. van der Tol, P. K. E. Campbell, and E. M. Middleton. 2020. "Fluorescence Correction Vegetation Index (FCVI): A Physically Based Reflectance Index to Separate Physiological and Non-Physiological Information in Far-Red Sun-Induced Chlorophyll Fluorescence." *Remote Sensing of Environment* 240: 111676. https://doi.org/10.1016/j.rse.2020.111676.

Zeng, Y., G. Badgley, M. Chen, J. Li, L. D. L. Anderegg, A. Kornfeld, Q. Liu, et al. 2020. "A Radiative Transfer Model for Solar Induced Fluorescence Using Spectral Invariants Theory." *Remote Sensing of Environment* 240: 111678. https://doi.org/10.1016/j.rse.2020.111678.

Zeng, Y., G. Badgley, B. Dechant, Y. Ryu, M. Chen, and J. A. Berry. 2019. "A Practical Approach for Estimating the Escape Ratio of Near-Infrared Solar-Induced Chlorophyll Fluorescence." *Remote Sensing of Environment* 232: 111209. https://doi.org/10.31223/osf.io/3w9nz.

Zhang, C., J. Atherton, J. Peñuelas, I. Filella, P. Kolari, J. Aalto, H. Ruhanen, J. Bäck, and A. Porcar-Castell. 2019. "Do all Chlorophyll Fluorescence Emission Wavelengths Capture the Spring Recovery of Photosynthesis in Boreal Evergreen Foliage?" *Plant, Cell & Environment* 42: 3264–79. https://doi.org/10.1111/pce.13620.

## SUPPORTING INFORMATION

Additional supporting information can be found online in the Supporting Information section at the end of this article.

**How to cite this article:** Pierrat, Zoe Amie, Troy Magney, Andrew Maguire, Logan Brissette, Russell Doughty, David R. Bowling, Barry Logan, Nicholas Parazoo, Christian Frankenberg, and Jochen Stutz. 2024. "Seasonal Timing of Fluorescence and Photosynthetic Yields at Needle and Canopy Scales in Evergreen Needleleaf Forests." *Ecology* e4402. https://doi.org/10.1002/ecy.4402